

**UNIVERSIDADE FEDERAL DE MINAS GERAIS**  
**Instituto de Geociências**  
**Programa de Pós-Graduação em Geologia**

Matheus Fontana de Lima

**TRACE ELEMENTS IN SEDIMENTARY PYRITE TRACK REDOX AND  
NUTRIENT FLUCTUATIONS IN THE EDIACARAN/CAMBRIAN BAMBUÍ  
GROUP, BRAZIL.**

**Nº 248**

Belo Horizonte  
2023

Matheus Fontana de Lima

**TRACE ELEMENTS IN SEDIMENTARY PYRITE TRACK REDOX AND  
NUTRIENT FLUCTUATIONS IN THE EDIACARAN/CAMBRIAN BAMBUÍ  
GROUP, BRAZIL.**

Dissertação apresentada ao Programa de Pós-Graduação em Geologia da Universidade Federal de Minas Gerais como requisito parcial para obtenção do título de Mestre em Geologia.

Orientador(a): Prof. Dr. Fabrício de Andrade  
Caxito

Belo Horizonte  
2023

L732t  
2023

Lima, Matheus Fontana de.

Trace elements in sedimentary pyrite track redox and nutrient fluctuations in the Ediacaran/Cambrian Bambuí Group, Brazil [manuscrito] / Matheus Fontana de Lima. – 2023.

56 f., enc. il. (principalmente color.)

Orientador: Fabrício de Andrade Caxito.

Dissertação (mestrado) – Universidade Federal de Minas Gerais, Instituto de Geociências, 2023.

Área de concentração: Geologia Regional.

Bibliografia: f. 50-56.

1. Piritas – Teses.
  2. Sedimentos (Geologia) – Brasil – Teses.
  3. Gondwana (Geologia) – Teses.
- I. Caxito, Fabrício de Andrade. II. Universidade Federal de Minas Gerais. Instituto de Geociências. III. Título.

CDU: 551.3.051(81)



UNIVERSIDADE FEDERAL DE MINAS GERAIS

PROGRAMA DE PÓS-GRADUAÇÃO EM GEOLOGIA DO IGC-UFMG



## FOLHA DE APROVAÇÃO

**TRACE ELEMENTS IN SEDIMENTARY PYRITE TRACK REDOX AND NUTRIET FLUCTUATIONS IN THE EDIACARAN/CAMBRIAN BAMBUÍ GROUP, BRAZIL**

**MATHEUS FONTANA DE LIMA**

Dissertação submetida à Banca Examinadora designada pelo Colegiado do Programa de Pós-Graduação em GEOLOGIA, como requisito para obtenção do grau de Mestre(a) em GEOLOGIA, área de concentração GEOLOGIA REGIONAL, pelo Programa de Pós-graduação em Geologia do Instituto de Geociências da Universidade Federal de Minas Gerais.

Aprovada em 04 de abril de 2023, pela banca constituída pelos membros:

*Fabrício de A. Caxito*

Prof. Dr. Fabrício de Andrade Caxito – Orientador

UFMG

*GJU*

Prof. Dr. Gabriel Jubé Uhlein

UFMG

*mfb*

Profa. Dra. Anelize Manuela Bahniuk Rumbelsperger

UFPR

Belo Horizonte, 04 de abril de 2023.

## **AGRADECIMENTOS**

Chega ao fim esta longa jornada e mais uma etapa da minha vida acadêmica. Ser estudante de mestrado no Brasil não é fácil, principalmente nos últimos anos, mas eu tive a sorte de ter ao meu lado pessoas que, com seu amor à ciência, competência e apoio, tornaram essa caminhada mais prazerosa. Não poderia deixar de ser grato à todas elas.

Primeiramente, agradeço ao meu orientador, Fabrício Caxito, pela oportunidade de tê-lo como parceiro neste trabalho, pelas discussões geológicas e por não medir esforços para este estudo acontecer. Mas o mais importante, pela compreensão durante esse período tão difícil que foi a pandemia do covid-19, que foi um grande obstáculo a ser vencido para o desenvolvimento deste trabalho.

Também agradeço aos(as) geólogos(as) cujas contribuições foram essenciais para esta pesquisa: Luana Duarte, Lucas Lana e William Moura, aos co-autores do artigo produzido, que elevaram bastante o nível com suas ponderações, e aos pesquisadores Ross Large e Indrani Murkhejee, responsáveis pelo tratamento das amostras na University of Tasmania.

Obrigado ao programa de pós-graduação em Geologia do IGC-UFMG e à Pró-reitoria de Pós-graduação (PRPg) da UFMG, ao Centro de Pesquisas Professor Manoel Teixeira da Costa e aos técnicos dos laboratórios do IGC e ao nosso secretário da pós-graduação, William Viegas, pela paciência e atenção com todos os alunos do nosso curso.

Esse trabalho foi possível devido ao suporte da Universidade Federal de Minas Gerais (UFMG), do Programa de Pós-graduação em Geologia (PPGEOL), do Instituto de Geociências (IGC), do Departamento de Geologia, do CPMTC-IGC, da Fundação de Amparo à Pesquisa do Estado de Minas Gerais (FAPEMIG, processo PPM-00618-18), do Conselho Nacional de Desenvolvimento Científico e Tecnológico (CNPq, processo 408815/2021-3) e do Instituto Serrapilheira (Serra-1912-31510), através do Project MOBILE: Mountains Belts and the Inception of Complex Life on Earth ([geolifemobile.com](http://geolifemobile.com)).

Por fim, agradeço às pessoas mais importantes da minha vida: meus pais Angélica e Ronaldo e à minha noiva Luana. Obrigado por todo o sacrifício que já realizaram para que eu pudesse chegar até aqui. O apoio e o amor incondicional de vocês são meu combustível e tudo só terá sentido se eu tiver vocês ao meu lado. Amo vocês.

## **RESUMO**

A variação de Elementos Traço (TE) em piritas sedimentares, determinada pelo método LA-ICP-MS (Laser Ablation – Inductively Coupled Plasma Mass Spectrometry), tem o potencial de fornecer informações sobre diversas condições do ambiente marinho ao longo do tempo. Neste estudo, foi realizada a análise de Elementos Traço em piritas sedimentares do Grupo Bambuí. Destaca-se, no conjunto de dados, a mudança das concentrações de Mo, Se, Cu, Cd, Zn, Ni e Bi nas amostras do Membro Pedro Leopoldo em relação às concentrações destes elementos nas piritas das Formações Serra de Santa Helena e Lagoa do Jacaré, o que pode indicar restrição progressiva da bacia, passando de uma totalmente conectada para uma bacia restrita. As amostras de pirita do Membro Pedro Leopoldo estudadas neste trabalho mostram enriquecimentos de Mo de várias centenas de ppm, indicando um importante, embora passageiro, pulso de oxigenação como consequência da glaciação Marinoana. Uma camada óxica rasa provavelmente foi mantida até o final do Ediacarano, durante a deposição do Membro Lagoa Santa (585-540 Ma). No entanto, mudanças radicais nas concentrações de Mo e baixas concentrações gerais de micronutrientes são registradas na Formação Serra de Santa Helena, com níveis de O<sub>2</sub> bastante. Isso indica o desenvolvimento de águas ferruginosas em um cenário pobre em sulfato, devido à restrição da bacia pelas montanhas Brasilianas circundantes que formaram o Gondwana. As condições restritas, pobres em oxigênio e empobrecidas em nutrientes, causaram o desaparecimento de formas de vida complexas e prejudicaram o desenvolvimento de ecossistemas típicos do Ediacarano-Cambriano. A religação da bacia pode ter ocorrido durante a deposição da Formação Lagoa do Jacaré, com maiores quantidades O<sub>2</sub> no ambiente. Os resultados destacam a importância da restrição e conexão da bacia sobre as variações da disponibilidade de nutrientes durante o desenvolvimento dos ecossistemas Ediacaranos-Cambrianos.

**Palavras-chave:** Pirita sedimentar. Elementos traço. Oxigenação atmosférica. Gondwana. Grupo Bambuí.

## ABSTRACT

The TE variation in sedimentary pyrites, determined by the LA-ICP-MS (Laser Ablation – Inductively Coupled Plasma Mass Spectrometry) method, has the potential to provide information on different conditions of the marine environment over time. In this study, the analysis of Trace Elements in sedimentary pyrites of the Bambuí Group was carried out. What stood out most in the data set was the change in concentrations of Mo, Se, Cu, Cd, Zn, Ni and Bi in the samples from the Pedro Leopoldo Member in relation to the concentrations of these elements in the pyrites of the Serra de Santa Helena and Lagoa do Jacaré, which may indicate progressive restriction of the basin, changing from a fully connected basin to a restricted basin. The pyrite samples from the Pedro Leopoldo Member shows Mo enrichments of several hundred ppm, indicating an important, albeit transient, pulse of oxygenation as a consequence of the Marinoan glaciation. A shallow oxic layer was probably maintained until the end of the Ediacaran, during the deposition of the Lagoa Santa Member (585-540 Ma). However, radical changes in Mo concentrations and low overall micronutrient concentrations are recorded in the Serra de Santa Helena Formation, with high O<sup>2</sup> levels. This indicates the development of ferruginous waters in a sulfate-poor setting, due to the restriction of the basin by the surrounding Brasiliana mountains that formed Gondwana. The restricted conditions, poor in oxygen and depleted in nutrients, caused the disappearance of complex life forms and hindered the development of ecosystems typical of the Ediacaran-Cambrian. The reconnection of the basin may have occurred during the deposition of the Lagoa do Jacaré Formation, with greater amounts of O<sup>2</sup> in the environment. The results highlight the importance of basin restriction and connection on variations in nutrient availability during the development of Ediacaran-Cambrian ecosystems.

**Keywords:** Sedimentary pyrite. Trace elements. Atmospheric oxygenation. Gondwana. Bambuí Group.

## LISTA DE FIGURAS

Figura 1.Imagem de satélite do estado de Minas Gerais, com a localização das amostras e as respectivas cidades próximas (Google Earth Pro, 2023).....	13
Figura 2.Fotografias de luz refletida (a, b, d) e microscopia eletrônica de varredura (c) de algumas das piritas sedimentares estudadas. A) Amostra JJ1 (mount); B) amostra MH-2; C) Amostra JJ1; D) Amostra MJ002. A Figura 2c mostra um grão composto de pirita. A zona externa do grão é euédrica e provavelmente pós-deposicional, mas essa borda não foi analisada. O miolo do grão é framboidal e é justamente essa porção central que foi analisada. ....	15
Figura 3. Presença do fóssil-guia do Ediacarano <i>cloudina</i> sp. Foto do autor, na região de Januária-MG.....	18
Figura 4. Localização da bacia do Bambuí no Gondwana (a) e no Cráton do São Francisco (b); (c) e (d) mapas geológicos das áreas estudadas com localização das amostras coletadas; (e) Coluna estratigráfica esquemática do Grupo Bambuí com posicionamento das amostras. ....	19
Figura 5. Diferenciação dos tipos de ambientes do Grupo Bambuí, realizado por método de especiação de ferro (retirado de Hippert et al., 2019). As amostras analisadas neste estudo estão situadas próximas a Januária-MG.....	20

## **LISTA DE TABELAS**

Tabela 1. Coordenadas dos locais de onde foram retiradas as amostras estudadas.....	12
Tabela 2.Divisão Litoestratigráfica do Grupo Bambuí, proposta por Dardenne (1978b, 1979) e ambientes de sedimentação segundo Dardenne (1981).....	16

## SUMÁRIO

<b>1. INTRODUÇÃO E FUNDAMENTAÇÃO .....</b>	<b>10</b>
<b>1.1. OBJETIVO .....</b>	<b>11</b>
<b>1.2. METODOLOGIA.....</b>	<b>11</b>
<b>1.2.1. REVISÃO BIBLIOGRÁFICA.....</b>	<b>11</b>
<b>1.2.2. AMOSTRAGEM .....</b>	<b>11</b>
<b>1.2.3 LOCALIZAÇÃO DAS AMOSTRAS.....</b>	<b>12</b>
<b>2. ANÁLISE DE ELEMENTOS TRAÇO EM PIRITAS POR LA-ICP-MS .....</b>	<b>14</b>
<b>3. CONTEXTO GEOLÓGICO .....</b>	<b>16</b>
<b>4. RESULTADOS.....</b>	<b>21</b>
<b>5. CONCLUSÃO .....</b>	<b>49</b>
<b>6. REFERÊNCIAS BIBLIOGRÁFICAS.....</b>	<b>52</b>

## 1. INTRODUÇÃO E FUNDAMENTAÇÃO

Quando se trata de rastrear as condições paleoambientais, entender os ambientes de sedimentação das rochas que compõem a paisagem atual e assim, compreender melhor a história do nosso planeta, a pirita sedimentar aparece como uma ferramenta única, uma vez que esse mineral incorpora Elementos Traço (TE). A variação de TE em piritas sedimentares, determinada pelo método LA-ICP-MS (Laser Ablation – Inductively Coupled Plasma Mass Spectrometry), tem o potencial de fornecer informações sobre diversas condições do ambiente marinho ao longo do tempo, como disponibilidade de bionutrientes, teor de enxofre, variações de pH, eventos de oxigenação, eventos anóxicos e atividade hidrotermal (Large et al., 2014; 2022). Esses, por sua vez, podem ser usados para interpretar as variações dos principais fatores biogeoquímicos ao longo do tempo geológico que desempenharam papéis centrais no desenvolvimento de ecossistemas complexos (Mukheerje e Large, 2020).

O Grupo Bambuí apresenta um registro geológico privilegiado para estudar a relação entre os sistemas biológicos, sedimentares, orogênicos e químicos do planeta Terra durante o Ediacarano/Cambriano, um momento chave na história geológica que testemunhou extremos climáticos, biológicos, tectônicos e mudanças *redox*, pois contém extensas sucessões sedimentares desta idade dominadas por rochas clásticas e químicas.

Neste trabalho, são apresentados dados sobre a variação de TE em piritas sedimentares de folhelhos negros, *chert* e rochas carbonáticas do Grupo Bambuí. O objetivo é discutir as relações entre as variações da disponibilidade de TE nesta importante unidade ediacarana/cambriana ao longo do tempo juntamente com as mudanças paleoclimáticas e paleoambientais. Além disso, o Grupo Bambuí representa um cenário único durante a transição Ediacarana/Cambriana, com episódios de restrição e conexão de bacia e re-ligações aos oceanos globais (Paula-Santos et al., 2017; Hippert et al., 2019; Uhlein et al., 2019, 2021; Caxito et al., 2021; Caetano-Filho et al., 2021; Guacaneme et al. al., 2022). Assim, estudar as variações de *proxies* químicos, como concentrações e proporções de TE em pirita ao longo da estratigrafia do Grupo Bambuí, pode fornecer informações importantes sobre como esses indicadores responderam a condições conectadas *versus* restritas em bacias antigas.

Esta pesquisa faz parte do Projeto MOBILE ([geolifemobile.com](http://geolifemobile.com)), uma rede internacional de cientistas que visa estudar as ligações entre cadeias de montanhas e o aparecimento da vida complexa na Terra, e conta com o apoio do Instituto Serrapilheira, do CNPq, e de universidades ao redor do globo. Destaca-se a colaboração com cientistas da

UNESP, UFMG e University of Tasmania (UTAS), que permitiram as análises realizadas aqui através da disponibilização de amostras e laboratórios.

### **1.1. OBJETIVO**

O trabalho apresenta como objetivo principal quantificar as concentrações de elementos traço em piritas sin-sedimentares de amostras de rocha do Grupo Bambuí. Através destes dados, são discutidas as relações entre as variações de disponibilidade de Elementos Traço bioessenciais e das condições *redox*, ao longo do tempo, com as mudanças paleoclimáticas e paleoambientais registradas no paleocontinente São Francisco.

### **1.2. METODOLOGIA**

A metodologia adotada para elaboração desta tese englobou diversas etapas e materiais que podem ser divididos em etapas de laboratório e escritório. As etapas de laboratório consistiram no levantamento e descrição das amostras cedidas, confecção de lâminas e *mounts* polidos, com o apoio da estrutura do CPMTC/UFMG, análise microscópica, documentação fotográfica e envio de algumas selecionadas para a UTAS, onde se submeteram ao LA-ICP-MS. Já as etapas de escritório incluíram levantamentos bibliográficos, tratamento dos dados obtidos e confecção do artigo e desta tese.

#### **1.2.1. REVISÃO BIBLIOGRÁFICA**

O levantamento bibliográfico correspondeu à primeira etapa do trabalho e se prolongou até o fim. Ele teve como objetivo o entendimento geológico do Grupo Bambuí de maneira geral, seu contexto na Geologia global e do Brasil, suas variações regionais, dados geocronológicos e conteúdo fossilífero.

#### **1.2.2. AMOSTRAGEM**

Para a realização deste trabalho, foram selecionadas amostras de carbonatos, siltitos, folhelhos negros e *cherts* das Formações Sete Lagoas, Serra de Santa Helena e Lagoa do Jacaré, que compõem o Grupo Bambuí. A maioria das amostras aqui estudadas foram previamente estudadas para análise de TE e especiação de ferro por Hippertt et al. (2019), e compreende folhelhos negros do membro Pedro Leopoldo da seção Holcim (HCX), um siltito do membro Pedro Leopoldo da seção Ilcon (MH3), siltitos da Formação Serra de Santa Helena na seção Papagaios (MH-2) e folhelhos negros da Formação Lagoa do Jacaré na pedreira Jaíba (MJ002). Para complementar este conjunto de dados, foi incluída a amostra JJ1, de um *chert* intercalado

com o carbonato Pedro Leopoldo na região de Januária (Okubo et al., 2018), amostras P26 e P1CL de calcários pretos da Formação Lagoa do Jacaré próximo à cidade de Unaí (Moura et al., 2022) e amostras de calcários pretos da Formação Lagoa do Jacaré na pedreira GMD (Freitas et al., 2021; Dantas et al., 2022). Seções finas e *mounts* polidos foram preparados para todas as amostras e a pirita sedimentar foi identificada e fotografada por microscopia óptica e eletrônica de varredura no Centro de Pesquisa Manoel Teixeira da Costa, Universidade Federal de Minas Gerais (CPMTC-UFMG) e Universidade Estadual Paulista (UNESP). É importante ressaltar que esta opção de buscar amostras de outros estudos foi uma alternativa à impossibilidade de realizar trabalhos de campo devido à pandemia do COVID-19.

Posteriormente, as melhores amostras foram selecionadas e enviadas para os laboratórios da University of Tasmania (UTAS), na Austrália, onde foram analisadas sob a responsabilidade dos pesquisadores Ross Large e Indrani Mukherjee através do método LA-ICP-MS. Apenas agregados de pirita que possuíam hábito framboidal foram selecionados para análise, e vários dados foram obtidos em cada agregado de pirita, a partir dos quais as concentrações médias de cada elemento traço foram calculadas.

### **1.2.3 LOCALIZAÇÃO DAS AMOSTRAS**

As amostras analisadas neste estudo, pertencentes ao Grupo Bambuí, estão todas localizadas no estado de Minas Gerais. As amostras GMD, MH e HCX estão localizadas próximas a Sete Lagoas, P26 e P1CL estão próximas a Ubaí, JJ1 está localizada em Januária e a amostra MJ está ao norte de Jaíba (Tabela 1 e Figura 1).

*Tabela 1. Coordenadas dos locais de onde foram retiradas as amostras estudadas.*

<b>Amostra</b>	<b>Latitude</b>	<b>Longitude</b>
HCX	-19.605223	-44.059066
JJ1	-15.428702	-44.396355
MH	-19.35241	-44.775167
GMD	-19.251607	-44.390181
MJ	-15.12395	-43.54266
P26	-16.199284	-44.762698

P1CL	-16.217889	-49.116809
------	------------	------------

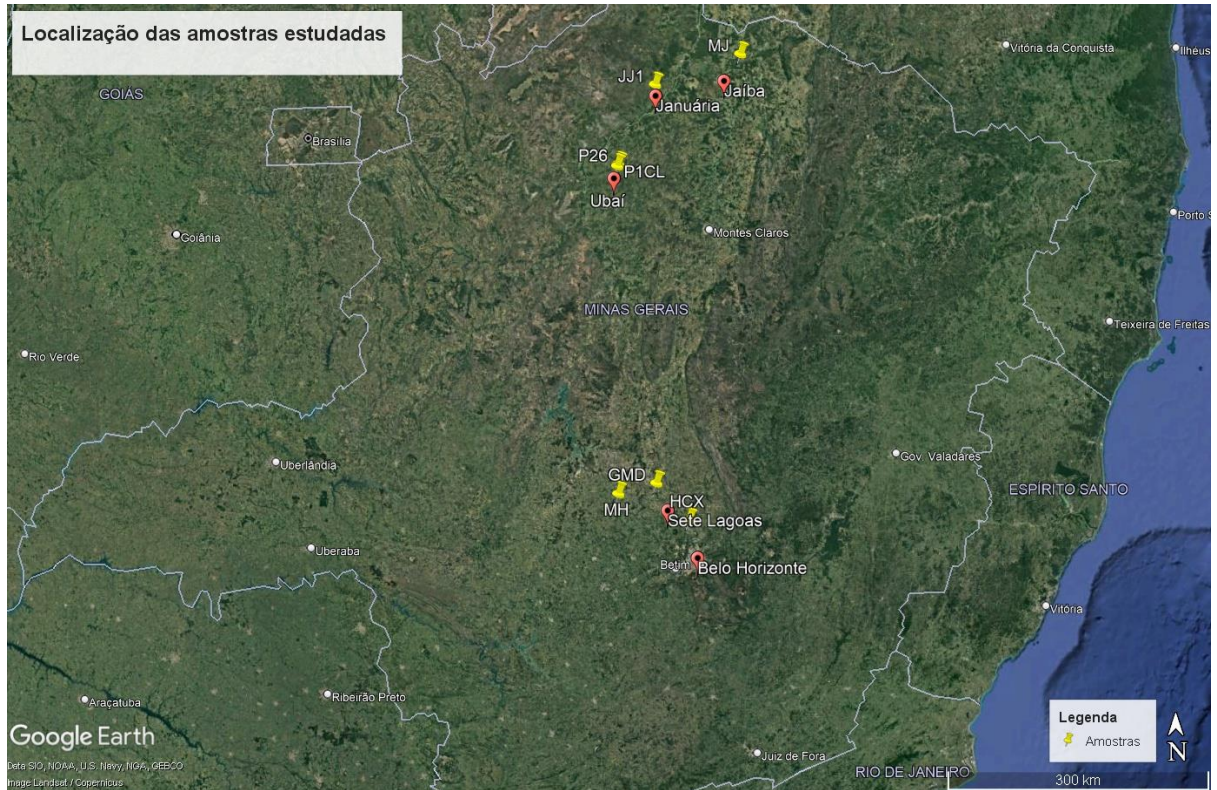


Figura 1. Imagem de satélite do estado de Minas Gerais, com a localização das amostras e as respectivas cidades próximas (Google Earth Pro, 2023).

## 2. ANÁLISE DE ELEMENTOS TRAÇO EM PIRITAS POR LA-ICP-MS

A análise de variação de Elementos Traço (TE) em folhelhos negros depositados em ambientes marinhos traz bons resultados para interpretar às condições paleo-redox do assoalho oceânico, incluindo mudanças temporais na oxigenação do paleo-oceano (Large *et al.*, 2014). E a maioria destes TE estão concentrados em piritas, FeS<sub>2</sub> (Huerta-Diaz, 1992; Large *et al.*, 2014).

A pirita sedimentar é formada no fundo dos oceanos quando o ácido sulfídrico, H<sub>2</sub>S, produto das atividades microbiais com o sulfato presente no ambiente marinho, reage com o Fe. Estas piritas recém-formadas incorporam TE, como: As, Hg, Mo, Co, Cu, Mn, Ni, Zr, Pb, Zn e Cd (Large *et al.*, 2007). Este processo de enriquecimento é controlado pela quantidade de TE disponíveis e a quantidade de FeS<sub>2</sub> produzida (Huerta-Diaz e Morse, 1992). No entanto, é reconhecido que este fato é um processo bioquímico complexo, e variáveis como o pH da coluna d'água e de sedimentos e descrescimento da bioprodutividade vão influenciar quais TE serão incorporados às piritas (Kulp e Pratt, 2004).

A textura é essencial para identificar os melhores pontos para análise, devendo-se escolher grãos e agregados de pirita que foram menos propensos a serem afetados por diagênese e outros tipos de alteração pós-deposicional. Piritas framboidais formadas dentro da coluna de água na Bacia euxínica de Cariaco (Piper e Dean, 2002; Lyons et al., 2003) têm TE que se aproximam de uma relação linear quando plotadas contra as concentrações médias modernas de TE de água oceânica (Large et al., 2014, 2019), apoiando a ideia de que o teor destes elementos na pirita formada sob condições euxínicas na coluna de água reflete o próprio teor da coluna de água na qual eles se formaram. Certamente, a química da pirita pode ser alterada com o grau de diagênese e metamorfismo. Essas variações podem, no entanto, ser detectadas e contabilizadas, e as análises que representam claramente um alto grau de sobreposição diagenética podem ser excluídas dos conjuntos de dados usados para a interpretação da química oceânica.

Neste foram selecionados grãos de pirita, agregados e núcleos de grãos compostos com evidência de menor impacto por diagênese, evidenciado por suas texturas primárias. Como análises múltiplas foram feitas para múltiplos agregados ou grãos de pirita de cada seção fina ou montagem polida, as análises que eram claramente discrepantes e fora do desvio padrão médio, possivelmente devido a efeitos diagenéticos ou de mistura de fases, foram excluídas do conjunto de dados.

O LA-ICP-MS combina a alta resolução espacial das sondas a laser com elevada sensibilidade, baixos limites de detecção e capacidade para análises multi-elementares (Allan *et. al.*, 2005). Resumidamente, nessa metodologia, a amostra é vaporizada através do LA e transportada pelo gás de arraste (argônio) para o interior do ICP onde os íons são criados e acelerados. Os íons entram, então, no espectrômetro de massa onde são separados por sua razão massa/carga. E, finalmente, são encaminhados a um detector que converte os sinais obtidos em espectros (Longerich *et. al.*, 1996).

Neste trabalho, um total de 13 amostras de piritas framboidais foram analisadas através do LA-ICP-MS na UTAS. O equipamento tem capacidade para analisar os seguintes elementos e seus respectivos isótopos:  $^{13}\text{C}$ ,  $^{23}\text{Na}$ ,  $^{24}\text{Mg}$ ,  $^{27}\text{Al}$ ,  $^{29}\text{Si}$ ,  $^{34}\text{S}$ ,  $^{39}\text{K}$ ,  $^{43}\text{Ca}$ ,  $^{49}\text{Ti}$ ,  $^{51}\text{V}$ ,  $^{53}\text{Cr}$ ,  $^{55}\text{Mn}$ ,  $^{57}\text{Fe}$ ,  $^{59}\text{Co}$ ,  $^{60}\text{Ni}$ ,  $^{65}\text{Cu}$ ,  $^{66}\text{Zn}$ ,  $^{75}\text{As}$ ,  $^{77}\text{Se}$ ,  $^{85}\text{Rb}$ ,  $^{88}\text{Sr}$ ,  $^{90}\text{Zr}$ ,  $^{95}\text{Mo}$ ,  $^{107}\text{Ag}$ ,  $^{111}\text{Cd}$ ,  $^{118}\text{Sn}$ ,  $^{121}\text{Sb}$ ,  $^{125}\text{Te}$ ,  $^{137}\text{Ba}$ ,  $^{157}\text{Gd}$ ,  $^{178}\text{Hf}$ ,  $^{181}\text{Ta}$ ,  $^{182}\text{W}$ ,  $^{195}\text{Pt}$ ,  $^{197}\text{Au}$ ,  $^{202}\text{Hg}$ ,  $^{205}\text{Tl}$ ,  $^{206}\text{Pb}$ ,  $^{207}\text{Pb}$ ,  $^{208}\text{Pb}$ ,  $^{209}\text{Bi}$ ,  $^{232}\text{Th}$  and  $^{238}\text{U}$ .

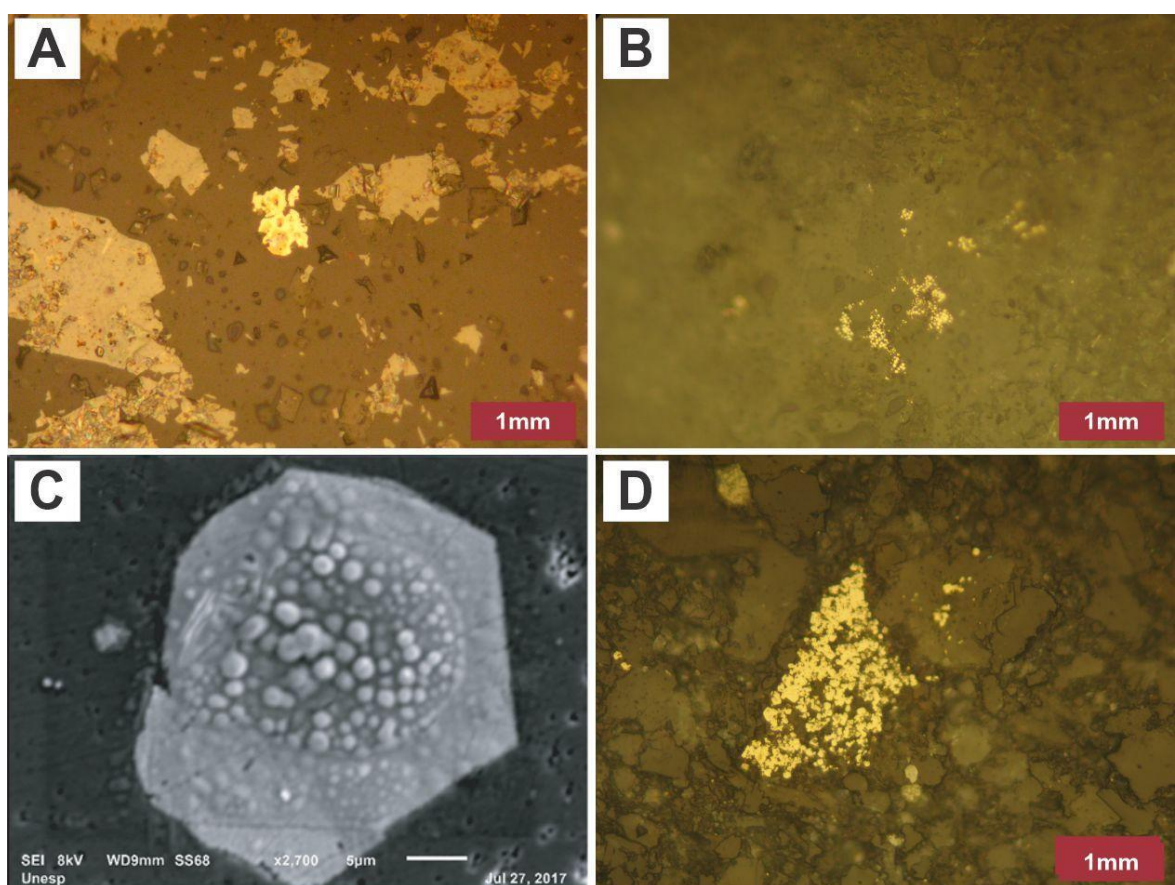


*Figura 2.*Fotografias de luz refletida (a, b, d) e microscopia eletrônica de varredura (c) de algumas das piritas sedimentares estudadas. A) Amostra JJI (mount); B) amostra MH-2; C) Amostra JJI; D) Amostra MJ002. A Figura 2c mostra um grão composto de pirita. A zona externa do grão é euhédrica e provavelmente pós-deposicional, mas essa borda não foi analisada. O miolo do grão é framboidal e é justamente essa porção central que foi analisada.

### 3. CONTEXTO GEOLÓGICO

A Bacia do São Francisco é uma bacia intracratônica levemente deformada na parte central e deformada em suas bordas devido às tensões compressivas do Orógeno Ediacarano Brasília, a oeste, e do Orógeno Ediacarano/Cambriano Araçuaí, a leste (Caxito et al., 2021 e referências nele contidas) Sua principal unidade estratigráfica é o Grupo Bambuí (Uhlein, 2013), que exibe a maior área de afloramentos dentre todas as unidades (Dardenne, 1978) e é composto por litofácies carbonato-siliciclásticas que representam uma extensa plataforma marinha com transição para um ambiente continental no topo.

A deposição do Grupo Bambuí é interpretada como tendo ocorrido principalmente em uma bacia de antepaís, devido à flexão por soterramento proveniente da erosão dos orógenos Brasília e Araçuaí (Caxito et al., 2012, 2021; Reis e Suss, 2016; Uhlein et al., 2017; Uhlein et al., 2019). Na porção centro-norte da Bacia, o embasamento gnáissico aflora em janelas estratigráficas através de um alto estrutural, o chamado Alto de Januária (Uhlein, 2013).

Em um dos trabalhos mais relevantes até hoje, Dardenne (1978a, 1979) propôs a litoestratigrafia mais aceita para o Grupo Bambuí na região do Brasil Central, contendo seis formações: Jequitaí, Sete Lagoas, Serra de Santa Helena, Lagoa do Jacaré, Serra da Saudade e Três Marias (Tabela 2).

*Tabela 2. Divisão Litoestratigráfica do Grupo Bambuí, proposta por Dardenne (1978b, 1979) e ambientes de sedimentação segundo Dardenne (1981).*

Formação	Litologia	Espessura (m)	Ambiente de Sedimentação
Três Marias	Siltitos, arenitos e arcóseos.	~100	Fluvial, marinho a sublitorâneo, marinho litorâneo.
Serra da Saudade	Folhelhos, argilitos e siltitos carbonáticos esverdeados.	25 - 200	Fluvial, marinho a sublitorâneo, marinho litorâneo.
Lagoa do Jacaré	Calcários políticos e psolíticos, siltitos, margas.	0-100	Marinho litorâneo.
Serra de Santa	Folhelhos e siltitos cinzas.	220-150	Marinho sublitorâneo.

Helena			plataforma.
Sete Lagoas	Calcários dolomíticos. Dolomitos, oólitos e estromatólitos.	250-200	Marinho sublitorâneo. plataformal.
Jequitaí	Paraconglomerados, dolomitos, cherts, gnaisses, micaxistos, granitos e rochas vulcânicas.	0-20	Glacial.

Outras unidades regionalmente importantes foram posteriormente descritas, como por exemplo as cunhas conglomeráticas das formações Samburá e Lagoa Formosa na porção oeste da bacia (Uhlein et al., 2017) e os carbonatos da Formação Jaíba na porção leste (Uhlein et al., 2021).

A Formação Jequitaí é composta por diamictitos glaciais e fácies relacionadas reposando sobre pavimentos estriados (Isotta et al., 1969) e é interpretada como relacionada à glaciação marinoana global (Caxito et al., 2012, 2018; Alvarenga et al., 2014 ; Crockford et al., 2018; Uhlein et al., 2019; Okubo et al., 2018). A Formação Sete Lagoas sobrejacente é subdividida em dois membros. O basal, Membro Pedro Leopoldo, compreende uma típica sucessão carbonática da base do Ediacarano, com uma unidade de dolomito irregular de poucos metros de espessura (Shields, 2005). Este dolomito de capa é seguido por um calcário de algumas centenas de metros de espessura contendo pseudomorfos de calcita após leques de cristais de aragonita (Vieira et al., 2007; Caxito et al., 2012, 2018; Alvarenga et al., 2014; Kuchenbecker et al., 2016; Uhlein et al., 2019; Caetano Filho et al., 2020) e incluindo depósitos de fosforita (Drummond et al., 2015), cimentos apatíticos (Okubo et al., 2018) e camadas centimétricas de barita (Crockford et al., 2018).

Acima do membro Pedro Leopoldo, o membro Lagoa Santa, com duzentos metros de espessura, compreende um segundo nível de calcário em leque cristalino sobreposto por estromatólitos laminares e colunares e trombólitos. O membro Lagoa Santa localmente contém vestígios fósseis de *Cloudina sp.* (Figura 3), conchas e fragmentos de *Corumbella werneri* (Warren et al., 2014).



*Figura 3. Presença do fóssil-guia do Ediacarano *cloudina* sp. Foto do autor, na região de Januária-MG.*

Subindo na estratigrafia, os valores de  $\delta^{13}\text{C}$  sobem rapidamente para  $> + 10\text{\textperthousand}$ , anormalmente altos em comparação com as curvas globais de água do mar Ediacara e persistem por cerca de 350 m, abrangendo a Formação Serra de Santa Helena dominada por siltitos e calcários da Formação Lagoa do Jacaré, e definindo a Excursão do Médio Bambuí (MIBE; Uhlein et al., 2019).

Os valores  $87\text{Sr}/86\text{Sr}$  também se desacoplam das curvas globais compiladas da água do mar Ediacarano-Cambriano, apresentando valores anormalmente baixos de  $<0,7075$  (Caxito et al., 2021; Guacaneme et al., 2021). Finalmente, a Formação Três Marias, dominada por arenitos, representa a sedimentação final do Grupo Bambuí e abrangeu o início do Cambriano, conforme sugerido pela ocorrência de *Treptichnus pedum* (Sanchez et al., 2021). Os valores dos isótopos de carbono e estrôncio tornam-se reacoplados às curvas globais da água do mar, sugerindo a reconexão da bacia do Bambuí (Caxito et al., 2021).

As restrições de idade disponíveis sugerem que o carbonato do Membro Pedro Leopoldo foi depositado após a glaciação Marinoana, com idades U-Pb em leques de cristais de calcita-aragonita em 621-600 Ma (Caxito et al., 2021). Já o membro Lagoa Santa, com *Cloudina*, foi depositado em torno de 585-540 Ma, de acordo com dados de zircônio detritico (Paula-Santos et al., 2015) e dados U-Pb calcita-aragonita (Caxito e outros, 2021). A datação de zircão, por U-Pb, provendo a idade de 520 Ma em um tufo da Formação Serra da Saudade (Moreira et al., 2020) fornece uma restrição de idade direta para o Grupo Bambuí superior. Assim, o Grupo Bambuí abrange todo o Ediacarano e atinge o início do Cambriano em suas porções superiores, tornando-se um excelente laboratório natural.

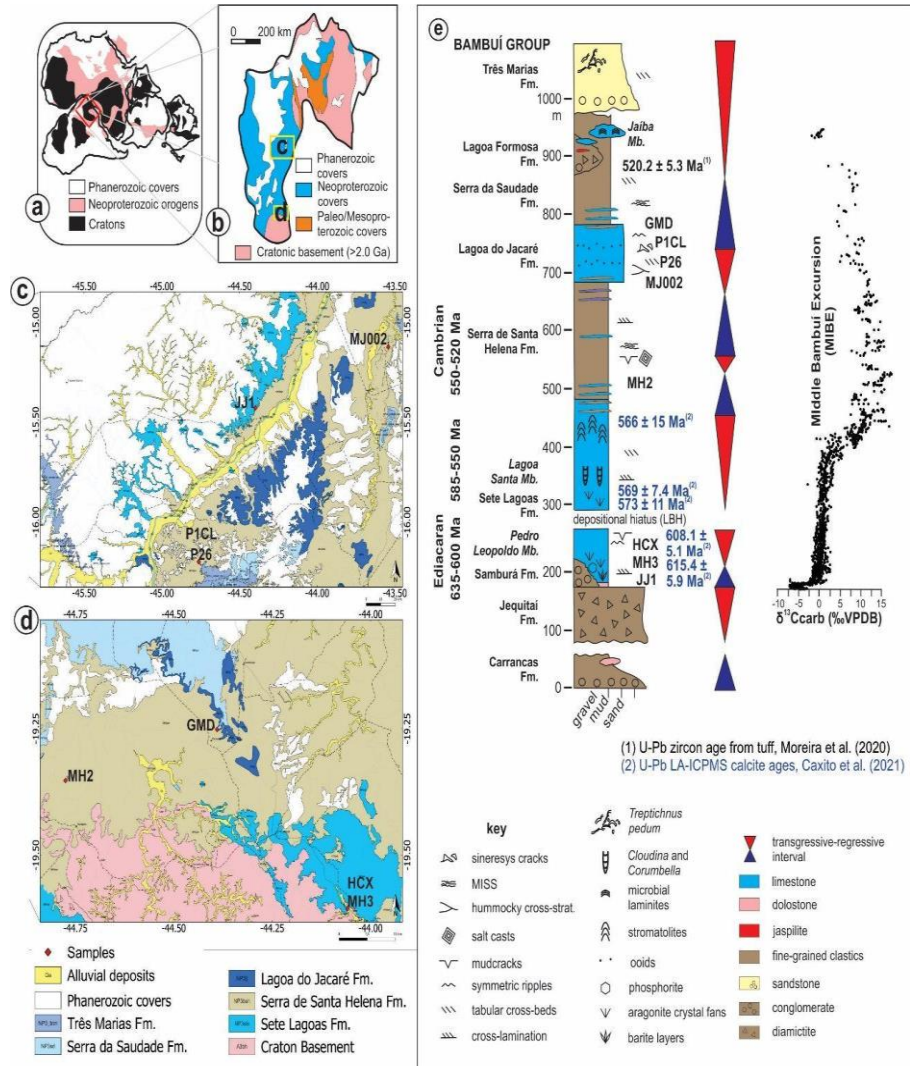


Figura 4. Localização da bacia do Bambuí no Gondwana (a) e no Cráton do São Francisco (b); (c) e (d) mapas geológicos das áreas estudadas com localização das amostras coletadas; (e) Coluna estratigráfica esquemática do Grupo Bambuí com posicionamento das amostras.

Em relação a estudos recentes que buscaram entender a variação vertical de bionutrientes da Bacia Bambuí e o tipo de ambiente de sedimentação, e se relacionam com este trabalho, destaca-se Hippert et al., (2019), que, mesmo que de maneira muito preliminar, através de métodos de especiação de ferro, definiram a transição de um ambiente óxico representado pela Fm. Sete Lagoas, para um ambiente anóxico representado pela Fm. Lagoa do Jacaré, porém com pequenas intercalações óxico/anóxico entre esse intervalo. Neste trabalho, os autores ainda definiram como um ambiente ferruginoso para toda a estratigrafia da bacia, porém poucas amostras foram analisadas (Figura 5). Caxito et al. (2021) reconheceram um aumento de cinco vezes, em carbonatos, de micronutrientes como Ba, Ni, Cu e Zn do membro Pedro Leopoldo para o membro Lagoa Santa, e sugeriram uma influência da erosão dos cinturões circundantes das montanhas Brasilianas desenvolvidas durante esse intervalo para a entrada, através do fluxo

fluvial, desses elementos na bacia.

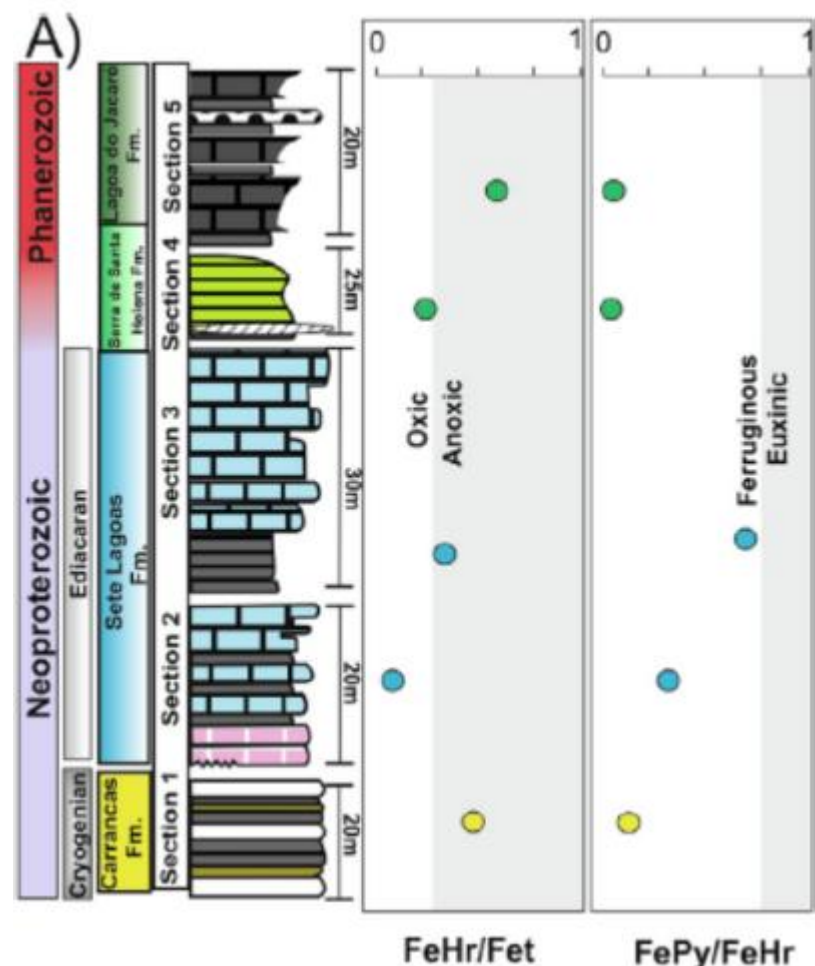


Figura 5. Diferenciação dos tipos de ambientes do Grupo Bambuí, realizado por método de especiação de ferro (retirado de Hippert et al., 2019). As amostras analisadas neste estudo estão situadas próximas a Januária-MG.

## 4. RESULTADOS

Os resultados deste trabalho foram submetidos em forma de artigo ao periódico Chemical Geology, na íntegra a seguir.

### **Trace Elements in Sedimentary Pyrite Track Redox and Nutrient Fluctuations in the Ediacaran/Cambrian Bambuí Group, Brazil**

Matheus F. de Lima<sup>1</sup>, Fabrício A. Caxito<sup>1</sup>, Ross Large<sup>2</sup>, Indrani Mukherjee<sup>2</sup>, Gabriel J. Uhlein<sup>1</sup>, João Pedro T.M. Hippertt<sup>3</sup>, Samuel A. Moura<sup>1</sup>, Juliana Okubo<sup>4</sup>, Lucas Warren<sup>4</sup>

1 CPMTC Research Center and Programa de Pós-graduação em Geologia, Universidade Federal de Minas Gerais, Belo Horizonte, MG 31270-901, Brazil

2 CODES ARC Centre of Excellence in Ore Deposits, University of Tasmania, Australia

3 Programa de pós-graduação em Evolução Crustal e Recursos Minerais, Departamento de Geologia, Universidade Federal de Ouro Preto, Ouro Preto, MG 35400-000,

Brazil

4 Department of Geology, São Paulo State University – UNESP, Rio Claro, SP 13506-900, Brazil.

#### **Abstract**

We apply trace element analysis of syn-sedimentary pyrite to track the redox and nutrient variations in the Ediacaran-Cambrian Bambuí Group of eastern Brazil. Sedimentary pyrite from black shales interleaved within the basal cap carbonate of the 635-600 Ma Pedro Leopoldo Member, deposited in an open marine setting connected to the global sea, preserve high Mo up to >200 ppm, erratic enrichment of micronutrients such as Cu, Ni, Ba, Zn and uniform enrichment of Se. This indicates the importance of oxidative continental weathering and development of an enhanced Redox Sensitive Elements (RSE) dissolved reservoir on the aftermath of the Marinoan glaciation, with atmospheric O<sub>2</sub> levels, calculated from Se/Co ratios of pyrites, around 2.5-3.5 wt%. A shallow oxic layer over deep euxinic realms made possible by high concentrations of dissolved sulfate was probably maintained up to the late Ediacaran, during deposition of the Cloudina-bearing Lagoa Santa Member (585-540 Ma). Upsection, however, radical shifts to muted Mo concentrations and overall low micronutrient concentrations are recorded in the Serra de Santa Helena Formation, with O<sub>2</sub> levels plunging below 1 wt%. This indicates the development of ferruginous bottom water conditions in a sulfate-poor setting, due to restriction of the basin by the encircling Brasiliano mountains that

formed Gondwana. The restricted, oxygen-poor and nutrient-depleted conditions caused the demise of complex life forms and hampered the development of typical Ediacaran-Cambrian ecosystems. Basin re-connection might have occurred during deposition of the Lagoa do Jacaré Formation, with higher calculated O<sub>2</sub> (up to ca. 7 wt%). Our results highlight the importance of basin restriction and connection over coupled redox-nutrients variations during the development of Ediacaran-Cambrian ecosystems.

## **Keywords**

Sedimentary pyrite, redox-sensitive elements, atmosphere oxygenation, Gondwana

### **1. Introduction**

Tracing ancient paleoceanographic conditions is essential to the development of integrated biogeochemical models of the Earth systems. In this context, sedimentary pyrite appears as a unique tool, as it concentrates fairly high amounts of redox-sensitive and nutrient Trace Elements (TE) (Gregory, et al., 2022). Sedimentary pyrite can be formed at the bottom of the oceans when hydrogen sulfide (H<sub>2</sub>S), as the product of microbial activities that consumes sulfate present in the marine environment, reacts with Fe. These syn-sedimentary pyrite incorporates TE such as As, Hg, Mo, Co, Cu, Mn, Ni, Zr, Pb, Zn and Cd (Large et al., 2007) and pore water. The enrichment process is controlled by the amount of TE available in the water column and by the amount of FeS<sub>2</sub> produced (Huerta-Diaz and Morse, 1992), through complex biochemical pathways influenced by variables such as pH of the water and sediment column and bioproduction levels (Kulp and Pratt, 2004). The variation of TE in sedimentary pyrites, determined in-situ by the LA-ICP-MS (Laser Ablation – Inductively Coupled Plasma Mass Spectrometry) method, has the potential to provide information about various conditions of the marine environment over time, such as availability of TE, sulfur content, pH variations, oxygenation events, anoxic events and hydrothermal activity (Large et al., 2014; 2022). Those, in turn, can be used to interpret variations of key biogeochemical factors through geological time, such as redox and nutrient conditions, which played central roles in the development of complex ecosystems (e.g. Mukheerje and Large, 2020).

The Bambuí Group in eastern Brazil presents a privileged geological record to test for feedback loops between the biological, sedimentary, orogenic and chemical systems of planet Earth during the Ediacaran/Cambrian, a key time in geological history that witnessed extreme climatic, biologic, tectonic and redox shifts in Earth systems, as it contains extensive sedimentary successions of this age dominated by both clastic and chemical rocks. In this

article, we present data on the variation of TE in sedimentary pyrites of black shale, chert and carbonate samples of the Bambuí Group (Figure 1). The objective is to discuss the relations between the variations of bio-essential trace elements availability in this important Ediacaran/Cambrian unit over time along with paleoclimatic and paleoenvironmental changes. Besides, the Bambuí Group represents a unique setting during the Ediacaran/Cambrian transition, with episodes of basin restriction due to the development of the mountain belts generated by orogenesis surrounding the São Francisco paleocontinent where it was deposited intercalated with episodes of basin connection and re-connection to the global sea waters (Paula-Santos et al., 2017; Hippert et al., 2019; Uhlein et al., 2019, 2021; Caxito et al., 2021; Caetano-Filho et al., 2021; Guacaneme et al., 2022). Thus, studying the variations of chemical proxies such as TE concentrations and ratios in pyrite throughout the Bambuí Group stratigraphy can yield important information on how those proxies responded to connected versus restricted conditions in ancient basins.

### **1.1. Geological Context**

The São Francisco Basin is an intracratonic basin slightly deformed or undeformed in the central part and deformed at its edges due to the compressional stresses from the Ediacaran Brasília Orogen, to the west, and the Ediacaran/Cambrian Araçuaí Orogen, to the east (Caxito et al., 2021, and references therein). Its main stratigraphic unit is the Ediacaran/Cambrian Bambuí Group (Figure 1), comprising mixed carbonate-siliciclastic lithofacies representing an extensive marine platform with the transition to a continental setting at the very top (uppermost Três Marias Formation). Deposition of the Bambuí Group is interpreted to have occurred mostly in a foreland basin setting, due to flexural loading of the developing Brasília and Araçuaí orogens over the cratonic margins (Caxito et al., 2012, 2021; Reis and Suss, 2016; Uhlein et al., 2017; Uhlein et al., 2019). The Bambuí Group comprises, from bottom to top: the Jequitaí, Sete Lagoas, Serra de Santa Helena, Lagoa do Jacaré, Serra da Saudade and Três Marias formations (Dardenne, 1978). Other regionally important units were further described and compose conglomeratic wedges of the Samburá and Lagoa Formosa formations in the western portion of the basin (Uhlein et al., 2017) and the Jaíba Formation carbonates in the eastern portion (Uhlein et al., 2021).

The Jequitaí Formation is composed of glacial diamictite and related facies resting atop striated pavements (Isotta et al., 1969) and is putatively interpreted as related to the global Marinoan glaciation (Caxito et al., 2012, 2018; Alvarenga et al., 2014; Crockford et al., 2018;

Uhlein et al., 2019; Okubo et al., 2018). The overlying Sete Lagoas Formation is subdivided into two members. The basal, Pedro Leopoldo Member comprises a typical early Ediacaran cap carbonate succession, with a meter-thick patchy cap dolostone unit (Shields, 2005) showing decreasing-upwards  $\delta^{13}\text{C}$  from -3.2‰ down to -6.5‰ and associated  $\delta^{18}\text{O}$  at -5‰ (Caxito et al., 2012). The cap dolostone is followed by a couple hundred meters-thick limestone containing pseudomorphs of calcite after original aragonite crystal fans with negative  $\delta^{13}\text{C}$  (Vieira et al., 2007; Caxito et al., 2012, 2018; Alvarenga et al., 2014; Kuchenbecker et al., 2016; Uhlein et al., 2019; Caetano Filho et al., 2020) and including phosphorite deposits (Drummond et al., 2015), apatitic cements (Okubo et al., 2018) and centimetric barite layers with a characteristic  $\Delta^{17}\text{O}$  anomaly (Crockford et al., 2018).  $^{87}\text{Sr}/^{86}\text{Sr}$  values show the characteristic early Ediacaran sharp peak from ca. 0.7074 to ca. 0.7080 (Caxito et al., 2021; Guacaneme et al., 2021), reflecting enhanced continental weathering (Halverson et al., 2010), suggesting that this cap carbonate succession was deposited under a water column connected to the global sea and recording global isotopic signals.

Above the Pedro Leopoldo member, the couple hundred meters-thick Lagoa Santa Member comprises a second crystal-fan-bearing limestone level with  $\delta^{13}\text{C}$  around 0‰, superimposed by laminar and columnar stromatolites and thrombolites with progressively higher  $\delta^{13}\text{C}$ . The Lagoa Santa member locally contains putative trace fossils and loosely packed *Cloudina sp.* shells and *Corumbella wernerii* fragments (Warren et al., 2014). Upwards, the  $\delta^{13}\text{C}$  values rise quickly to > + 10‰, anomalously high in comparison to late Ediacaran global seawater curves and persisting upsection for around 350 m, spanning the siltstone-dominated Serra de Santa Helena Formation and limestone of the Lagoa do Jacaré Formation. This isotopic anomaly is named Middle Bambuí Excursion (MIBE; Uhlein et al., 2019).  $^{87}\text{Sr}/^{86}\text{Sr}$  values also become decoupled from the global Ediacaran-Cambrian seawater compiled curves, presenting anomalously low values of <0.7075 (Caxito et al., 2021; Guacaneme et al., 2021), coeval with higher  $\epsilon\text{Nd(t)}$  values (Caxito et al., 2021). These unusual paleoenvironmental conditions might have prevailed up to the Cambrian Series 2, as suggested by a  $520.2 \pm 5.3$  Ma U-Pb zircon age of a tuff layer within the siltstone-dominated Serra da Saudade Formation (Moreira et al., 2020). Finally, the sandstone-dominated Três Marias Formation represents the final sedimentation of the Bambuí Group, and spanned the early Cambrian as suggested by the occurrence of *Treptichnus pedum* (Sanchez et al., 2021). Carbon and strontium isotope values become recoupled to the global seawater curves, suggesting reconnection of the basin to the global ocean (Caxito et al., 2021).

Available age constraints suggest that the Pedro Leopoldo cap carbonate was deposited after the Marinoan glaciation, with U-Pb LA-ICPMS ages on calcite-after-aragonite crystal fans at ca. 621-600 Ma (Caxito et al., 2021). The *Cloudina*-bearing Lagoa Santa member, on the other hand, was deposited around 585-540 Ma, according to detrital zircon data (Paula-Santos et al., 2015) and U-Pb calcite-after-aragonite data (Caxito et al., 2021). The aforementioned U-Pb LA-ICP-MS zircon age of ca. 520 Ma in an ash fall tuff of the Serra da Saudade Formation (Moreira et al., 2020) provides a direct age constraint for the upper Bambuí Group. Thus, the Bambuí Group spans the entire Ediacaran and reaches the early Cambrian in its upper portions, making it a prime natural laboratory to investigate Earth's biogeochemical cycles during this key time interval.

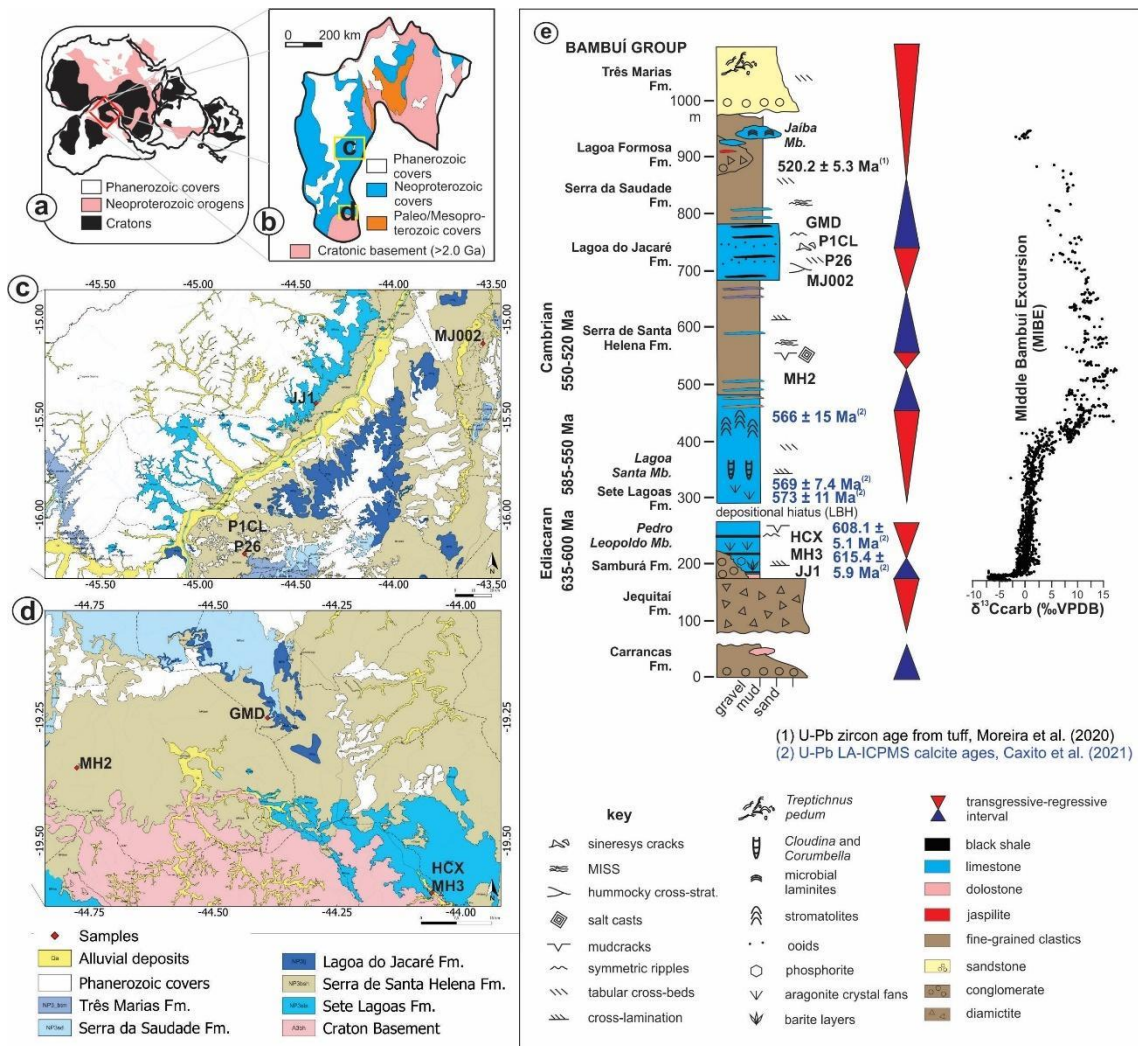


Figure 1 – Location of the Bambuí Group in Gondwana (a) and in the São Francisco Craton (b); (c) and (d) geological maps of the studied areas with location of the collected samples (see location of the maps in figure c); (e) Schematic stratigraphic column of the Bambuí Group with positioning of the studied samples. Carbon isotope data compilation in (e) and figures a, b and e modified from Caxito et al. (2021).

## 2. Materials and Methods

Most samples studied here (carbonates, siltstones, black shale and cherts from the Sete Lagoas, Serra de Santa Helena and Lagoa do Jacaré Formation) were previously analyzed for trace elements and iron speciation by Hippert et al. (2019), and comprise black shales of the Pedro Leopoldo member from the Holcim section (HCX,  $\text{Fe}_{\text{HR}}/\text{Fe}_{\text{T}} = 0.38$  and  $\text{Fe}_{\text{Py}}/\text{Fe}_{\text{HR}} = 0.6$ ), a siltstone of the Pedro Leopoldo member from the Ilcon section (MH3), siltstones from the Serra de Santa Helena Formation on the Papagaios section (MH-2,  $\text{Fe}_{\text{HR}}/\text{Fe}_{\text{T}} = 0.37$  and  $\text{Fe}_{\text{Py}}/\text{Fe}_{\text{HR}} = 0.03$ ) and black shale from the Lagoa do Jacaré Formation on the Jaíba quarry (MJ002,  $\text{Fe}_{\text{HR}}/\text{Fe}_{\text{T}} = 0.57$  and  $\text{Fe}_{\text{Py}}/\text{Fe}_{\text{HR}} = 0.15$ ). To complement this dataset, we included Sample JJ1, from a chert interleaved with the Pedro Leopoldo carbonate in the Januária region (Okubo et al., 2018), samples P26 and P1CL from black limestones of the Lagoa do Jacaré Formation near Unaí city (Moura et al., 2022) and samples from black limestones of the Lagoa do Jacaré Formation on the GMD quarry (Freitas et al., 2021; Dantas et al., 2022). Both thin sections and polished epoxy mounts were prepared for all of the samples and sedimentary pyrite was identified and imaged through optic and scanning electron microscopy at the Centro de Pesquisa Manoel Teixeira da Costa, Universidade Federal de Minas Gerais (CPMTC-UFMG) and Universidade Estadual Paulista (UNESP) laboratories (Figure 2).

Pyrite geochemistry analysis by LA-ICPMS is now a established method with various publications available, as summarized and described in great detail in Large et al. (2022). Texture is essential in identifying the best spots for analysis, in pyrite grains and aggregates that were less prone to be affected by diagenesis and other types of post-depositional alteration. In this respect, only pyrite aggregates that have a framboidal aspect were selected for analysis, while occasional euhedral individual grains or euhedral rims and overgrowths over framboidal aggregates were avoided. Pyrite framboids formed within the water column in the euxinic Cariaco Basin (Piper and Dean, 2002; Lyons et al., 2003) have trace elements that approximate a linear relationship when plotted against modern mean ocean water trace element concentrations (Large et al., 2014, 2019), supporting the idea that trace element content in pyrite formed under euxinic conditions in the water column reflect the trace element content of the water column in which they formed. Certainly, however, despite being a highly refractory and robust mineral able to retain chemical information, pyrite chemistry can be changed with the degree of diagenesis and metamorphism. These variations can, however, be detected and accounted for, and analyses that clearly represent a high degree of diagenetic overprint can be excluded from the datasets used for ocean chemistry interpretation. Previous studies of pyrite

from Neoproterozoic shales showed, for example, that based on texture, trace element composition of pyrites interpreted to be deposited at different periods of diagenesis tend to vary approximately by an order of magnitude (Large et al., 2007) whereas pyrite variations that indicate changes in ocean chemistry, vary through time by 2 to 4 orders of magnitude. In this study we selected pyrite grains, aggregates and cores of composite grains with evidence for the least impact by diagenesis, as evidenced by their primary textures. As multiple analyses were done for multiple pyrite aggregates or grains from each thin section or polished mount, analyses that were clearly discrepant and off the mean standard deviation, possibly due to either diagenetic or phase mixture effects, were excluded from the dataset.

Multiple pyrite grains and aggregates were analyzed from each sample, and various data points were obtained on each pyrite grain or aggregate, from which average concentrations of each trace element can be calculated. Data reduction techniques for pyrite and trace element analyses are discussed in Large et al. (2014, 2015, 2018, 2019), Mukherjee et al. (2018), and Stepanov et al. (2020). Both matrix and pyrite analyses were used in the data reduction process in order to account for mixing of pyrite and matrix components during LA-ICP-MS analyses of small pyrite grains. Initial data reduction techniques included an algorithm based on subtraction of the matrix component estimated from mass balance proved to show some limitations owing to subjectivity in selection of the pyrite and matrix compositions and difficulty in determining uncertainties. The data processing technique was modified by development of an Excel-based data reduction software developed in-house, which uses a linear regression-based algorithm for determining chalcophile and siderophile abundances relative to sulfur, for calculation of sulfide composition. The method has been outlined and discussed in Stepanov et al. (2020).

A total of 13 thin sections/epoxy mounts of rock samples containing framboidal pyrites were analyzed using the LA-ICP-MS facility at CODES, UTAS, with a laser beam diameter of diameter of 10-25 µm, depending on the size of pyrite grains. The facility is equipped with a New Wave Research UP-193ss laser microprobe coupled to an Agilent 7700s quadrupole ICP-MS. The facility has the capacity to analyse for the following elements and their respective isotopes, <sup>13</sup>C, <sup>23</sup>Na, <sup>24</sup>Mg, <sup>27</sup>Al, <sup>29</sup>Si, <sup>34</sup>S, <sup>39</sup>K, <sup>43</sup>Ca, <sup>49</sup>Ti, <sup>51</sup>V, <sup>53</sup>Cr, <sup>55</sup>Mn, <sup>57</sup>Fe, <sup>59</sup>Co, <sup>60</sup>Ni, <sup>65</sup>Cu, <sup>66</sup>Zn, <sup>75</sup>As, <sup>77</sup>Se, <sup>85</sup>Rb, <sup>88</sup>Sr, <sup>90</sup>Zr, <sup>95</sup>Mo, <sup>107</sup>Ag, <sup>111</sup>Cd, <sup>118</sup>Sn, <sup>121</sup>Sb, <sup>125</sup>Te, <sup>137</sup>Ba, <sup>157</sup>Gd, <sup>178</sup>Hf, <sup>181</sup>Ta, <sup>182</sup>W, <sup>195</sup>Pt, <sup>197</sup>Au, <sup>202</sup>Hg, <sup>205</sup>Tl, <sup>206</sup>Pb, <sup>207</sup>Pb, <sup>208</sup>Pb, <sup>209</sup>Bi, <sup>232</sup>Th and <sup>238</sup>U. To quantify the abundances of chalcophile elements, lithophile elements, and sulfur abundances, we used three standard reference materials. STGL2b2 (in-house reference material for calibration of relative element sensitivities; Danyushevsky et al., 2011) was used for chalcophile elements, GSD-1G

(USGS reference glass; Jochum et al., 2005) for silicates and a stoichiometric pyrite PPP-1 crystal (Gilbert et al., 2014) to sulfur. The three reference materials were analysed twice, before and thereafter, ~every 1.5 hours as well as at the beginning and end of a run. Background analyses for 30-seconds was acquired before the signal from the ablated sample was acquired for 40-60 seconds (~3.5 J/cm<sup>2</sup> laser fluence and 5 Hz laser repetition rate). Ablation took place in a He atmosphere, flowing at a rate of 0.8 l/min, along with mixing of the ablation stream with the Ar carrier gas (0.85 l/min). Raw data generated as counts per seconds for elements by LA-ICP-MS were processed using the latest version of LADR (CODES LAser Data Reduction software). Results are presented in the Supplementary Table S1.

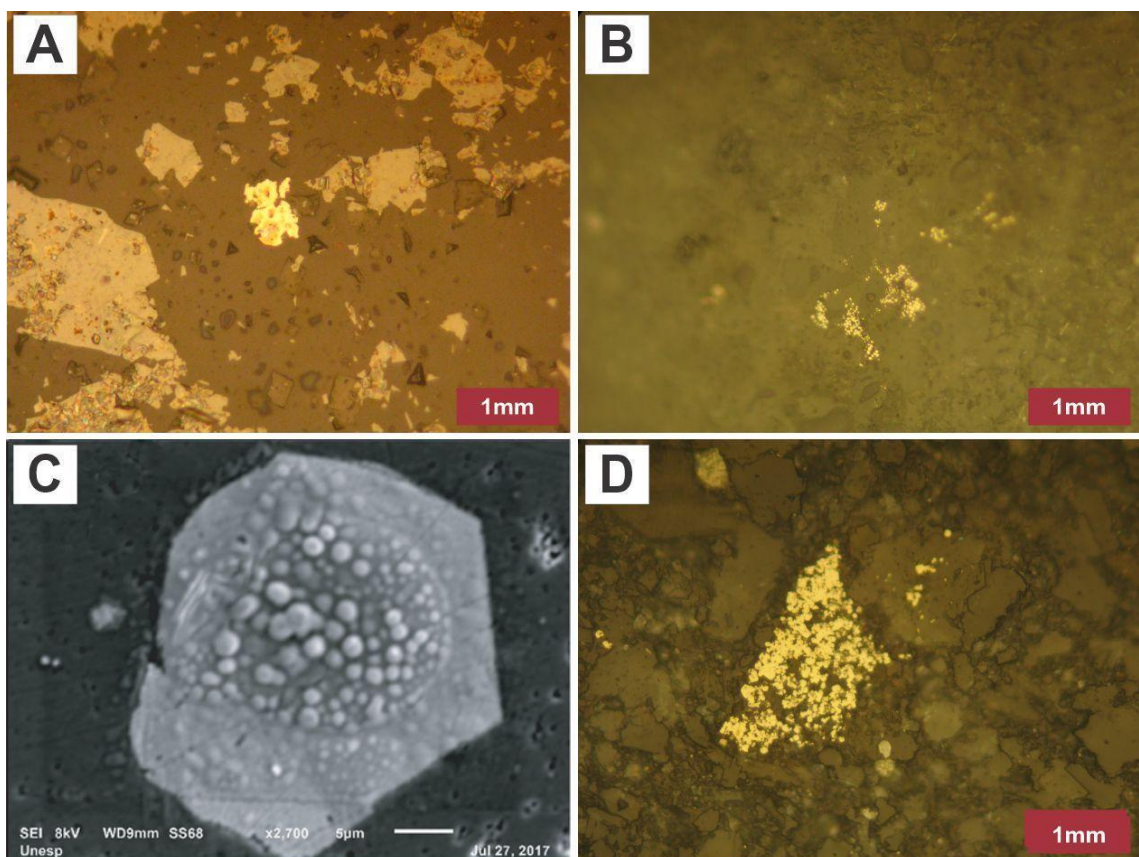


*Figure 2 – Reflected light (a, b, d) and scanning electron microscopy (c) photographs of some of the studied sedimentary pyrites. A) Sample JJ1 (mount); B) sample MH-2; C) Sample JJ1; D) Sample MJ002. Figure 2c shows a composite pyrite grain. The external zone of the grain is euhedral and probably post-depositional, but that rim was not analyzed. The core of the grain is frambooidal and it is precisely this central portion that was analyzed.*

### 3. Results and Discussion

Figure 3 shows the distribution of trace element contents and Se/Co ratios following Steadman et al. (2020). In the following sections, we discuss these results in terms of redox and nutrient variability in the different units that compose the Bambuí Group.

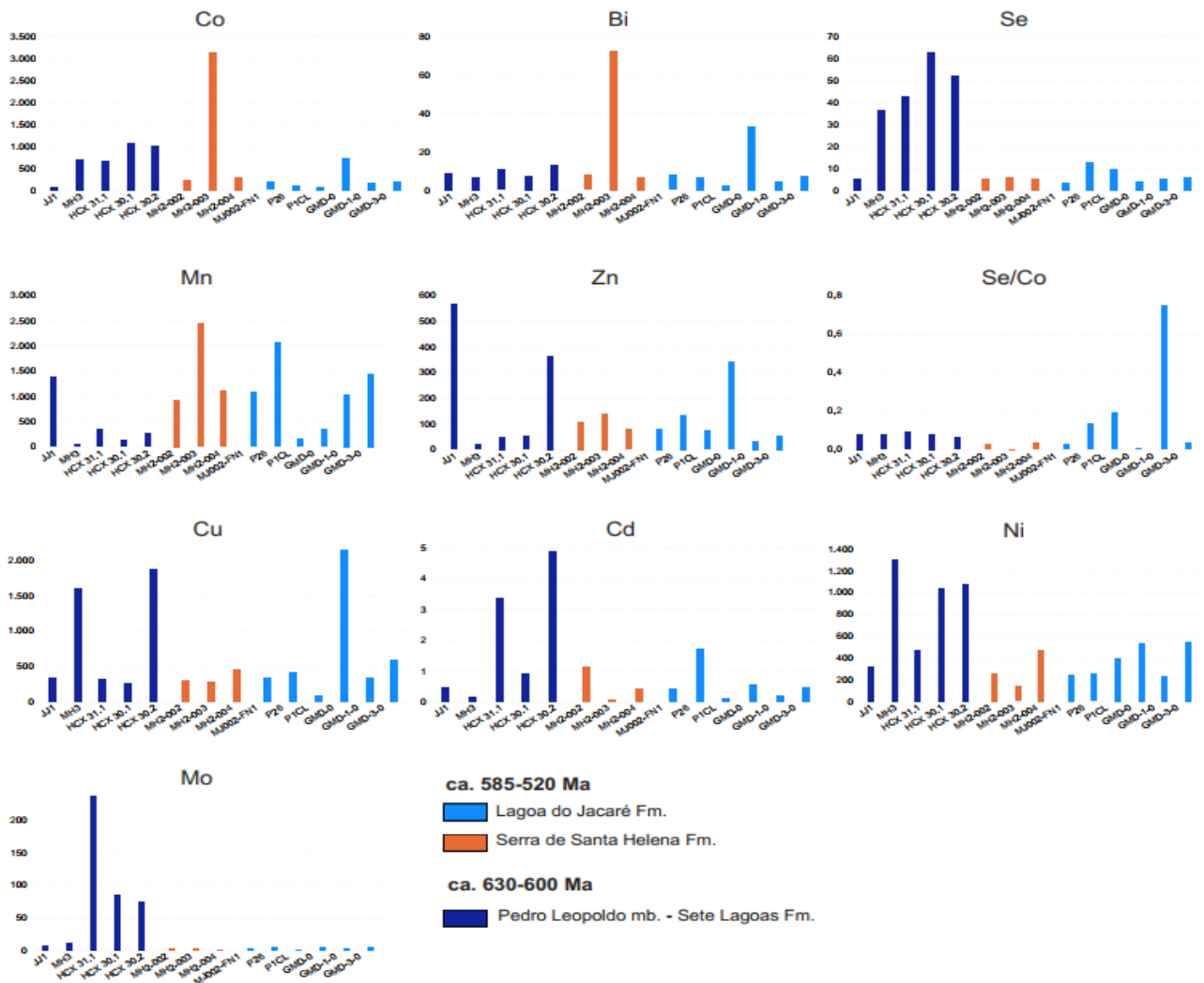


*Figure 3 – Obtained trace element data according to the stratigraphic positioning of samples from the Bambuí Group.*

### **3.1. A pulse of oxygenation on the aftermath of the Marinoan glaciation and the influence of basin restriction**

The most striking feature of the obtained dataset is the radical shift from enriched Mo, Se, Cd, Zn, Ni, Cu and Bi concentrations in pyrites from the early Ediacaran Pedro Leopoldo cap carbonate in relation to relatively depleted or practically muted (Mo, Se) concentrations in the Serra de Santa Helena and Lagoa do Jacaré Formations. Progressive basin restriction from a fully connected to a restricted basin due to diachronous development of the surrounding Brasiliano-aged mountain belts around the São Francisco craton (Brasília orogen at ca. 630-600 Ma followed by Araçuaí orogen at ca. 560-540 Ma, and finally by the terminal collisions of Gondwana at ca. 540-500 Ma; Caxito et al., 2021) is probably the main cause of

paleoenvironmental change, in line with various datasets such as decoupling of the  $\delta^{13}\text{C}$  and  $^{87}\text{Sr}/^{86}\text{Sr}$  values from the global seawater curve (Paula-Santos et al., 2017; Caxito et al., 2012, 2021; Uhlein et al., 2019; Cui et al., 2020; Caetano-Filho et al., 2020) and provenance shifts recorded by detrital zircon contents (Paula-Santos et al., 2015; Uhlein et al., 2017; Kuchenbecker et al., 2020; Caxito et al., 2021). The difference between the JJ1 sample in relation to the others in Pedro Leopoldo mb. is notable. It is possible that it is enriched in Zn due to the Pb-Zn mineralization reported by Nobre-Lopes (2002), since Ni, Co and Mo decrease with the proximity of hydrothermal vents (Mukherjee & Large, 2017).

The concentration of RSE in shales and other marine sedimentary rocks is dependent of a combination of factors. Oxic conditions on the continent and in surface waters are necessary for Mo mobilization and enrichment in the marine seawater reservoir, and oxidative weathering would essentially increase the availability of these elements in the water column. Then, euxinic conditions restricted to a small portion of the deeper ocean are necessary for scavenging of these elements into sedimentary rocks in local settings (Scott et al., 2008; Sahoo et al., 2012; Large et al., 2014). Therefore, higher concentrations of Mo or any other element that is sensitive to oxidative weathering can be used as proxy for higher atmospheric  $\text{pO}_2$ , but only if local euxinic conditions in the water column can ultimately promote scavenging of the dissolved enriched RSE seawater reservoir in sediments/shales.

In compilations of black shale data throughout geological time, higher concentrations of Mo interpreted as stemming from a higher input through oxidative weathering occurs after ca. 551 Ma (Scott et al., 2008). Pyrite samples from the Pedro Leopoldo Member studied in this paper show similar Mo enrichments of several hundred ppm but were deposited earlier, around 635-600 Ma ago (Caxito et al., 2021), indicating an important, albeit transient, oxidative weathering pulse in the aftermath of the Marinoan glaciation. Although direct comparison of trace metal concentrations between sedimentary pyrite and the host black shale whole rock is not feasible due to the potential amplification of the trace metal signals in the pyrite structure, most studies found that pyrite concentrations mirror those of the host black shales, faithfully pinpointing the same oxygenation events (Large et al., 2014; Gregory et al., 2019). In fact, the higher Mo contents were found in pyrites from the Holcim section black shale samples, which show the higher Mo enrichment factors found in the Bambuí Group (around 10 times those of Post Archean Australian Shale - PAAS; Hippertt et al., 2019). This interpretation is in line with Cr isotope compositions ( $\delta^{53}\text{Cr}$  up to  $+0.1\text{\textperthousand}$ ), Fe speciation ( $\text{Fe}_{\text{HR}}/\text{Fe}_{\text{T}} = 0.14$ ) and shale normalized Ce/Ce\* ratios down to 0.6 (Caxito et al., 2018, 2021; Hippertt et al., 2019) that

suggest transient pulses of oxygenation recorded in the Pedro Leopoldo Member. These oxygenation pulses, however, seem to have been protracted features of the early Ediacaran ocean, with more erratic conditions attained worldwide in Ediacaran-Cambrian basins before complete oxygenation of the global atmosphere-ocean system in the early Phanerozoic (Sperling et al., 2015; Sahoo et al., 2016; Caxito et al., 2018, 2022). In any case, oxidative weathering produced an expanded RSE-dissolved reservoir in the immediate post-glacial, globally connected waters where the Pedro Leopoldo Member was deposited. This is supported by recent N isotope data in bulk-rock samples (Fraga-Ferreira et al., 2021). Mo-based nitrogenase is an important enzyme used by microorganisms for N<sub>2</sub> fixation. The concentration of Mo in the water column can thus act as a limiting nutrient for certain biological pathways and influence N isotope values of sediment/rock samples. A sharp increase of  $\delta^{15}\text{N}$  from around +1 to ca. +5‰ in the Pedro Leopoldo cap carbonate supports biological N<sub>2</sub> fixation using Mo-based nitrogenase followed by the development of an expanded nitrate pool in surficial oxygenated waters (Fraga-Ferreira et al., 2021).

A recent study by Okubo et al. (2022) recorded high CAS (carbonate-associated sulfate) levels in the Pedro Leopoldo cap carbonate, and a major drawdown of sulfate upsection in the cap carbonate and persisting through the remainder of the Bambuí Group. This is coherent with the availability of sulfate from oxidative weathering in the stratified post-glacial ocean, with bacterial reduction generating enough H<sub>2</sub>S for the local development of euxinic bottom waters and growing of sedimentary pyrite that would incorporate trace metals, especially Mo, from the expanded RSE-dissolved reservoir. Upsection, however, CAS values plunge, and sulfur isotope systematics indicate sulfate-depleted conditions (Cui et al., 2020, Okubo et al., 2022). Evidence for bacterial sulfate reduction is provided by the sulfur isotope ratios preserved in those sediments and pyrites. Sulfate concentration can dictate the magnitude of S isotope fractionation between sulfate and sulfide (Cui et al., 2020). Also, the varying availability of sulfur (measured in the form of CAS) is linked with sulfur isotope ratios to show that lower sulfate levels in the upper Bambuí Group inhibited the activity of sulfur-reducing bacteria which in turn produces H<sub>2</sub>S, as recorded by coupled sulfate and sulfide S isotope variations (Cui et al., 2020; Okubo et al., 2022).

This leads to two possible scenarios for the muted RSE concentrations of sedimentary pyrite in the late Ediacaran-early Cambrian Serra de Santa Helena and Lagoa do Jacaré formations. First, with sulfate-depleted conditions, euxinia is not possible and, under ferruginous anoxic conditions, sedimentary pyrites might not record the true extent of the RSE-

dissolved reservoir, due to the lack of local settings with the proper euxinic conditions for scavenging of those RSE into the sediments (Scott et al., 2008). Indeed, the iron speciation results obtained by Hippert et al. (2019) suggest ferruginous conditions for both units, with  $\text{Fe}_{\text{HR}}/\text{Fe}_{\text{T}} = 0.37$  and 0.57 and  $\text{Fe}_{\text{Py}}/\text{Fe}_{\text{HR}} = 0.03$  and 0.15, respectively. Second, in restricted basins, hydrographic conditions such as relative stratification have larger influence on RSE concentrations in shales than redox conditions (Algeo and Rowe, 2012). For example, Mo concentrations in shales from the present-day Black Sea are only 3-5% that of the open sea (Algeo and Rowe, 2012), even though deposited under euxinic conditions. This can be possible because of the disconnection from the RSE-enriched pools with rare deepwater renewal on silled basins.

### **3.2. Quantification of oxygen levels in the Bambuí Group**

Of the various RSE that are incorporated into pyrite (including Ni, Co, As, Mo, Cu, Bi, Sb, Ag, Tl, Se and Te), those that are stoichiometrically held in the pyrite structure, and thus less affected by metamorphism and recrystallization, are Ni, Co and Se (Large et al., 2014). Under oxidizing conditions, Se is the most mobile of these with a residence time of 36,000 years, whereas Co is the least mobile with a residence time of only 340 years due to micronutrient uptake and scavenging processes (Saito et al., 2010), while Ni is in between with a residence time of 6,000 years (Nozaki, 2010; Large et al., 2022). Thus, both Se and Co are redox sensitive elements, but their different solution chemistry leads to opposite behavior according to oxygen levels. Co is absorbed and locked onto  $\text{Fe}^{3+}$  oxyhydroxides and  $\text{Mn}^{3+/4+}$  oxides under moderate to highly oxygenated conditions, but released by reductive dissolution as  $\text{Co}^+$  or  $\text{CoO}$  under reducing conditions (Stockdale et al., 2010; Steadman et al., 2020). On the other hand, Se becomes increasingly soluble as selenate ( $\text{SeO}_4^{2-}$ ) and selenite ( $\text{SeO}_3^{2-}$ ) species under oxygenated conditions, while under reducing conditions it is less mobile due to the insoluble nature of selenides ( $\text{H}_2\text{Se}$ ),  $\text{Se}^0$  and organo-selenium complexes (Mukherjee and Large, 2016).

The different behavior of Co compared to other RSE such as Mo and Se can be understood through the predominant ionic form of the soluble species. Cationic forms (such as the predominant soluble Co species,  $\text{Co}^{2+}$ ,  $\text{CoCl}$  or  $\text{CoO}$ ) show a great affinity for the  $\text{OH}^-$  ion, are scavenged by Fe-Mn hydroxides much more effectively, and are involved in complexation reactions with organic and inorganic ligands that play a major role in their sorption-desorption

processes, toxicity and phytoavailability (Violante et al., 2007, Mukheerje et al., 2019). Co in particular shows an exceptional affinity towards Mn hydroxides, which are much more efficient scavengers than Fe-Al hydroxides, in comparison to other TE (Murray, 1975; Violante et al., 2007). Mobility of anionic species (such as the predominant soluble Se species,  $\text{SeO}_4^{2-}$  and  $\text{SeO}_3^{2-}$ ) even though absorbed by metal oxides and allophones, mainly depends on available sites and/or reduction of the surface charge of the sorbents between trace elements and foreign ligands (Mukheerje et al., 2019).

The dominant source for dissolved RSE in the marine reservoir is riverine flux, where trace elements are transported in their soluble/particulate form (Scott et al., 2008; Sahoo et al., 2012; Algeo and Rowe, 2012; Large et al., 2014). Under oxidative weathering, Co will be released from pyrite in the continents as cationic species, which are immobilized by absorption on Mn and Fe oxides and hydroxides, while Se and other RSE are carried by the riverine flux as soluble anionic species to the seawater reservoir. Ultimately, both Co and Se are incorporated from the seawater reservoir in sedimentary pyrite on shales and other deep sea sedimentary rocks (Large et al., 2022). Under this rationale, Se/Co ratios in sedimentary pyrite have been proposed to be directly proportional to atmospheric O<sub>2</sub> through the following relationship:

$$\text{Atmospheric O}_2 \% = 30 \times P/(1+P)$$

$$\text{Where } P = 10^{[0.89 \times \log(\text{Se}/\text{Co}) + 0.07, r^2]}; r^2 = 0.85 \text{ (Steadman et al., 2020)}$$

The unique contrast between the long-term mobility of Se and Co under changing atmospheric oxygen levels delineates the Se/Co ratio as the main pyrite proxy (Large et al., 2015; Mukherjee and Large, 2016), varying through seven orders of magnitude due to trends of increasing and decreasing atmospheric oxygenation, and consequently of the flux of Se and Co to the oceans, across geological time (Large et al., 2019; Steadman et al., 2020). Recently (Canell et al., 2022) the Se/Co ratio in sedimentary pyrite has been calibrated and semi quantified using estimates of atmosphere oxygen by Blamey et al (2016), based on the gases trapped in fluid inclusions in sedimentary halite.

The uncertainty on the Se/Co ratios as calculated from Steadman's et al. (2020) formula is at  $\pm 3\%$  and does not affect interpretation of the data in the concentrations obtained. As the proxy is based on the availability of Se and Co through oxidative weathering on land, which are then transported to the basin, the proxy can be applied for both isolated and open marine settings, in order to estimate the amount of oxidative weathering that might have taken place in

the source areas independently of the nature of the final sink for those elements, if restricted or open. Besides, as discussed, not all of the Bambuí Group was deposited in a restricted setting. Only the middle portion of the group, corresponding to the MIBE anomaly of late Ediacaran age, is interpreted to have been deposited in such a setting. Thus, Se/Co ratios, along with other TE proxies, can probably record global geochemical signals both in the lower, early Ediacaran post-Marinoan portion of the Bambuí Group and in the upper, probably early Cambrian units.

Applying Steadman's et al. (2020) formula to Se/Co data from the Bambuí Group, early Ediacaran samples (~630 Ma) would yield relatively uniform atmospheric O<sub>2</sub> averaging 2.5 to 3.5 wt % ( $\pm 0.1$ ) or 0.12 to 0.17 PAL. On the other hand, the late Ediacaran to early Cambrian samples would first show a plunge, then a progressive increase of < 1% to ca. 7% ( $\pm 0.2$ ) average O<sub>2</sub> wt% towards the younger samples. While the results for the latter might seem at odds with the development of a restricted basin, those samples represent distinct sedimentary settings. The plunge to low Se/Co (low O<sub>2</sub>) characterize the Serra de Santa Helena Formation, whose mudstones and shales represent a major transgression and sample the deepest portions of the basin. A progressive sea-level drop is then observed upsection towards the shallow oolithic limestones of the Lagoa do Jacaré Formation, which shows tide-influenced sedimentary structures on the top (Moura et al., 2022), the highest Se/Co values and calculated O<sub>2</sub> wt% averaging ca. 7% ( $\pm 0.2$ ). Se/Co concentrations in pyrite might be roughly zoned across the basin from the near-shore shallow end out into the deep end, according to the different residence times of those elements. As discussed, Co has a comparably short residence time of 340 years and is more concentrated in the near shore carbonate bearing facies, whereas Se is more concentrated in the center of the basin, with a two orders of magnitude longer residence time of 36,000 years (Nozaki, 2010; Saito et al., 2010; Large et al., 2022). This means that calculated atmospheric oxygen levels using Steadman's et al. (2020) formula might be overestimated for the Lagoa do Jacaré Formation.

Alternatively, the influence of high-frequency tidal cycles in the Lagoa do Jacaré Formation might represent a return to at least partial oceanic connection in the Bambuí Group. In effect, fully restricted basins such as the Caspian and Black seas do not show relevant tidal influence (Levyant et al. 1994, Kulikov and Medvedev 2013, Medvedev *et al.* 2016), indicating that towards the top of the Lagoa do Jacaré Formation the Bambuí sea might have started to reconnect to the global sea through strait marine corridors (Moura et al., 2022). This is in line with: i) the waning stage of the MIBE anomaly (Cui et al., 2020) and the gradual return to more normal carbon cycle conditions observed on the top of the Lagoa do Jacaré Formation and in

the overlying Jaíba Member carbonates of the Serra da Saudade Formation (Uhlein et al., 2020); ii) the abundance of diagenetic glauconite (Moreira et al., 2019) and phosphatic beds in the overlying Serra da Saudade Formation, that suggests, respectively, suboxic conditions with availability of both Fe(II) and Fe(III) under a distinct Fe-sink mechanism from the pyrite-bearing Lagoa do Jacaré Formation, and upwelling of deep nutrient-rich waters (developed due to the high organic carbon burial rates during the preceding MIBE); and iii) the presence of putative *Treptchynus pedum* trace fossils on the topmost unit of the Bambuí Group (Sanchez et al., 2020), the Três Marias Formation, indicating the return of favorable conditions for colonization of complex life forms. In this scenario, the high Se/Co values observed on the Lagoa do Jacaré Formation might indeed represent a renewed oxygenation pulse in the Bambuí Group, although the quantification of represented atmospheric O<sub>2</sub> is complicated by the factors discussed above.

### **3.3. Nutrient variability on the Bambuí Group**

Caxito et al. (2021) recognized a five-fold increase, in bulk rock carbonates, of micronutrients such as Ba, Ni, Cu and Zn from the Pedro Leopoldo to the Lagoa Santa member, and suggested an influence of erosion from the surrounding Brasiliano mountain belts developed during this time frame on the riverine input of these TE to the basin. Unfortunately, samples from the Lagoa Santa member of the Sete Lagoas Formation were not analyzed in this study, due to the lack of proper sedimentary pyrites (all pyrites observed in samples from this unit are euhedral, as typical of diagenetic and hydrothermal pyrite, and were thus avoided for the objectives of this study). In this study, samples from the Serra de Santa Helena and Lagoa do Jacaré formations indicate that micronutrient conditions were more variable upsection. While higher concentrations of Co, Bi and Mn are observed in those samples most of the other TE are depleted in comparison to the Pedro Leopoldo samples, including important micronutrients such as Cd, Se, Zn, Ni, Cu and Mo.

Two possibilities can be proposed for the nutrient TE variations discussed above. First, nutrient delivery through erosion of the surrounding mountain belts was not as important during deposition of the Serra da Saudade and Lagoa do Jacaré formations than during deposition of the Lagoa Santa member, which coincides with the peak of orogenic deformation, magmatism and metamorphism in the surrounding fold belts (Caxito et al., 2021). This could help to explain the occurrence of complex life fossils such as *Cloudina* sp. in the Lagoa Santa member, during a period of optimum oxygen and nutrient conditions (Caxito et al., 2021); and their absence

upsection, first due to a possible eutrophication effect in the topmost Lagoa Santa member (Caxito et al., 2021), and afterwards due to a general shortage of nutrients in the following early Cambrian fully restricted basinal setting, after the peak of orogenic activity. This interpretation is consistent with  $\delta^{15}\text{N}$  data that for this interval of the Bambuí Group which indicate intercalated periods dominated by  $\text{N}_2$  fixation and  $\text{NO}_3^-$  assimilation, suggesting nitrate depletion as one of the factors that might have further affected conditions for metazoan evolution during the MIBE interval (Fraga-Ferreira et al., 2021).

Additionally, the overall absence of trace fossils in the Bambuí Group suggests that the lack of bioturbation also might have impacted the distribution and recycling of nutrients in the restricted phase of the basin. Scarcity of trace elements and limitation of their fixation under anoxic conditions might have impacted macronutrient availability, preventing the evolution of early benthic metazoans (Hippert et al., 2019; Guacaneme et al., 2022). Thus, even though feedbacks between the development of benthic organisms, development and decrease of the dissolved organic carbon pool, enhanced organic carbon burial and seawater oxygenation have been proposed (e.g. Tatzel et al., 2017), in the case of the Bambuí Group those factors were must probably overwhelmed by the impact of local basin restriction.

In sum, the discussed trace element, S and N variations within the Bambuí Group suggest that, while the basal, post-Marinoan cap carbonate succession might record oxygen and nutrient variations that reflect the global seawater conditions, interpretation of the upper, early Ediacaran to Cambrian units is contentious and highly difficulted by the restricted nature of the basin, disconnected from global seawater and representing a unique local Ediacaran-Cambrian setting. In any case, the available datasets indicate that after a peak of nutrient input coincident to the main phase of orogenic activity in the surrounding mountain belts, recorded in the lower to mid-portion of the Lagoa Santa Member, the Bambuí Group became stagnant, nutrient-depleted and dominated by anoxic (ferruginous) conditions, leading to development of the MIBE interval and the demise of any complex life forms during deposition of the upper Lagoa Santa Member, the Serra de Santa Helena Formation and the lower portion of the Lagoa do Jacaré Formation. Then, upsection, basin re-connection might have occurred as recorded in the upper Lagoa do Jacaré Formation, leading to more oxygenated conditions and the deposition of glauconite-rich sediments in the overlying Serra da Saudade Formation, and ultimately the return of complex life forms as recorded by putative trace fossils in the topmost Três Marias Formation.

### 3.4. Comparison to global sedimentary pyrite data

Our global LA-ICPMS sedimentary pyrite database (Large et al., 2014), has been used to demonstrate patterns in micro-nutrient concentrations in the global ocean through the Precambrian and Phanerozoic (Mukherjee and Large, 2020; Large et al., 2015). The Phanerozoic study suggested that five cycles, with the pattern low-high-low nutrients could be recognized from the pyrite trace element data, with the length of each cycle varying from 35 to 70 million years. Low points in the cycles contained episodes of major mass extinctions (end Ordovician, Late Devonian, end Permian and Jurassic-Triassic boundary), whereas high points corresponded to periods of significant biological evolution and radiation of species (Large et al., 2015). This cyclic pattern can also be recognized in sedimentary pyrite chemistry from Cryogenian to Early Cambrian (Fig 4). The first global cycle extends from about 660 to 645 Ma toward the end of the Cryogenian, the second cycle covers most of the Marinoan glaciation from 645 to 630 Ma, the third cycle is from 630 to 570 Ma corresponding to the evolution of the Ediacaran biota and the final Neoproterozoic cycle is from 570 to 500 Ma, including the extinction of the Ediacaran biota and the Cambrian explosion. The concentration of nutrient TE in pyrite gradually increases through the cycles, as indicated by the key micro-nutrient Se (Fig 4a) and the combined micro-nutrient factor (Fig. 4b). The peak in micro-nutrients in pyrite, and by proxy, the global ocean, occurs between 540 and 520 Ma, corresponding with the Cambrian explosion, when all major animal species evolved. It is significant that the pyrite proxy, used for atmospheric oxygen (Se/Co ratio), follows the same cyclic pattern and increases through the cycles to a maximum in the Early Cambrian (Fig. 4d).

The micro-nutrient pattern for sedimentary pyrite in the Bambuí Group shows some similarities, but significant differences to the global pyrite data (Fig. 4c). The cyclic pattern evident in the global dataset is not obvious from the Bambuí Group pyrite data, but this may be due to a lower number of measured samples for the latter. Except for two outlier samples (MH2-003 and GMD-3-0) there is a general decrease in micro-nutrients with stratigraphic height from Early Ediacaran to Early Cambrian. This pattern might be expected for a basin which became restricted from the global ocean in the mid to late Ediacaran, and did not become reconnected until the early Cambrian. We consider the pattern of generally decreasing nutrients, due to gradual drawdown of trace elements exceeding the replenishment by the erosive continental flux, to be the signature of a basin cut-off from the global ocean for an extended period.

On the other hand, the global ocean data indicates short periods of nutrient drawdown toward the end of each cycle (~643, ~630, ~580 and ~500 Ma; Fig. 4b), followed by a relatively rapid increase, possibly related to global orogenic mountain-building events which increase the nutrient flux (Campbell and Squire, 2010; Large et al., 2015; Zhu et al, 2022). The 35 to 70 million years cyclic nutrient pattern of the global ocean may be a critical feature of evolution and renewal, not only in the Phanerozoic (Large et al., 2015), but also the Neoproterozoic. Evolutionary processes may have been suppressed in highly restricted basins, due to a lack of continual renewal of critical life-supporting trace element nutrients (Hippert et al., 2019). This is supported by the general lack of late Ediacaran and early Cambrian macrofossils in the Bambuí Group above the Cloudina-bearing level (Warren et al., 2014).

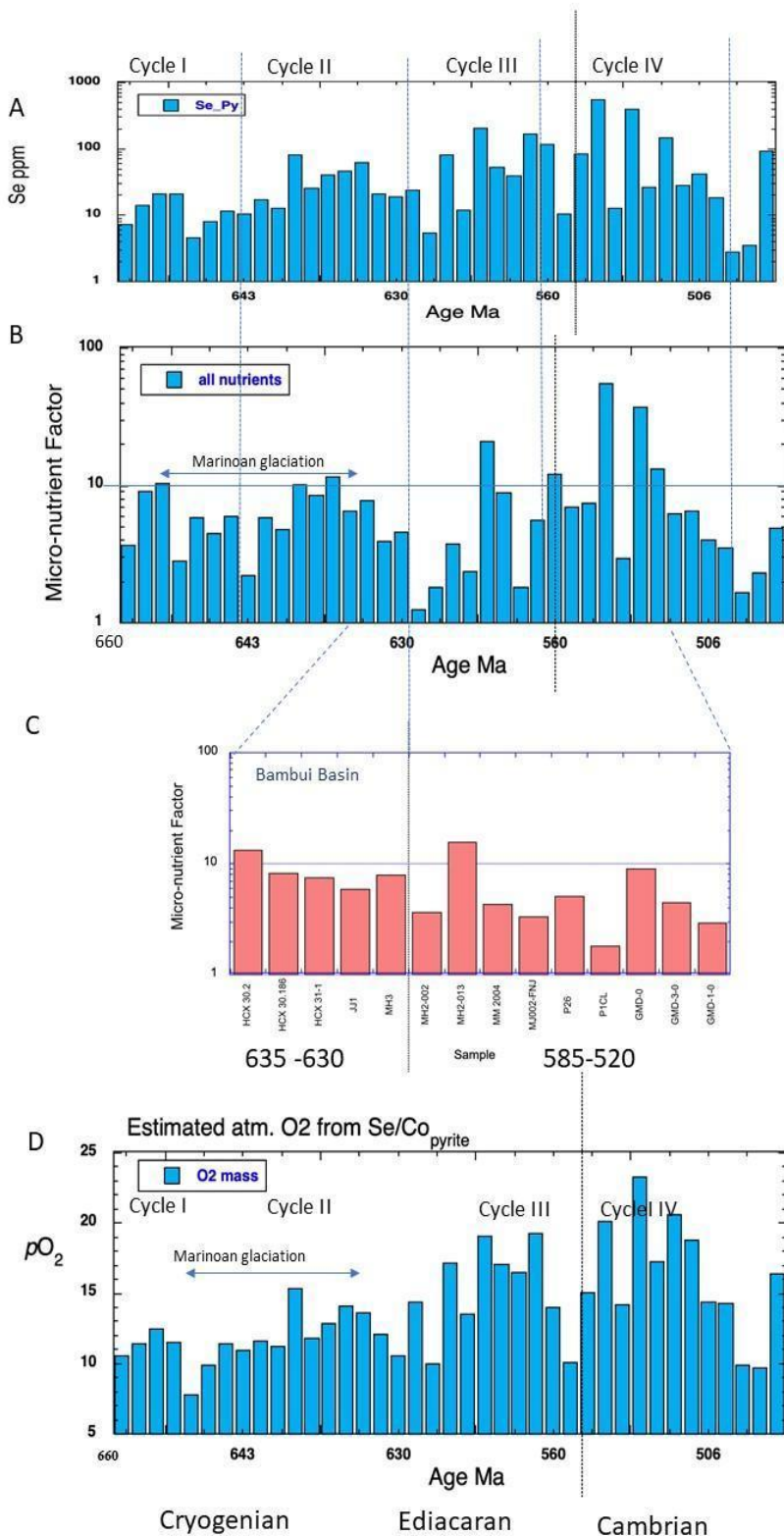


Figure 4 – Bar charts comparing the Bambuí Group data with the global database of sedimentary pyrite analysis. 4A: Bar chart of mean Se content in a global set of sedimentary pyrite (Large et al., 2022) between 660 and 500 Ma grouped in order of age. 4B: Bar chart of the micro-nutrient factor, determined as the cumulative value of the normalized Mo + Se + Cd + Zn + Cu + Mn + Co in sedimentary pyrite between 660 and 500 Ma grouped in order (Large et al., 2022). 4C: Bar chart of the micro-nutrient index for samples in this study from the Bambuí Basin. The index was calculated by the same method as in 4B. 4D: Bar chart of estimated pO<sub>2</sub>, for the global sedimentary pyrite set, calculated from the Se/Co ratio measured in pyrite.

#### 4. Conclusion

Trace element contents of sedimentary pyrite from black shale, siltstone, carbonate and chert samples of the Bambuí Group indicates radically distinct paleoenvironmental conditions during deposition of the basal, early Ediacaran post-Marinoan Pedro Leopoldo cap carbonate member and the late Ediacaran-early Cambrian units that compose the upper stratigraphic sections. Our results indicate the importance of basin connection and restriction on the concentration of TE in pyrite from stratigraphic units deposited during these distinct paleoenvironmental settings, and the influence of external forces such as orogenesis in the biogeochemical factors that can lead to development or damaging of complex marine ecosystems.

The Pedro Leopoldo cap carbonate was deposited in a platform connected to the global sea at ca. 635-600 Ma, under a stratified water column with a shallow oxic layer and deep locally euxinic settings. In consequence, sedimentary pyrite records an enhanced dissolved RSE marine reservoir, concentrated through oxidative weathering and riverine input and then scavenged and incorporated in sedimentary pyrite on the local euxinic settings. Se/Co ratios indicate relatively uniform atmospheric O<sub>2</sub> of 2.5 to 3.5 wt % ( $\pm 0.1$ ) on the aftermath of the Marinoan glaciation. The studied proxies clearly indicate oxygenated conditions upon deglaciation of the Snowball Earth; however, global evidence suggests that these represent transient, protracted atmospheric oxygenation pulses, and that Earth's atmosphere would only become unidirectionally oxygenated to modern levels much later in the early Phanerozoic. In any case, the transient oxygen and nutrient conditions were maintained up to the late Ediacaran, when fleeting colonization of biomimeticizing organisms such as *Cloudina* sp. occurred as recorded in the Lagoa Santa Member, deposited at ca. 585-540 Ma.

Upsection, however, the paleoenvironmental conditions radically changed, leading to muted RSE and erratic micronutrient contents in sedimentary pyrite of the late Ediacaran to early Cambrian Serra de Santa Helena and Lagoa do Jacaré formations. In agreement with other available proxies, this indicates the progressive restriction of the Bambuí Group and disconnection from the global ocean by the development of the surrounding Brasiliano mountain belts. Increased riverine input of nutrient TE is recorded in the Lagoa Santa Member of late Ediacaran age, roughly coincident with the peak of deformation, magmatism and metamorphism in the surrounding orogens, and might have led to eutrophication upon full restriction of the basin recorded by the onset of the MIBE anomaly. This positively fractionated

(up to ca. +15‰) carbon isotope anomaly spans ca. 350 meters of sedimentary successions including the upper Lagoa Santa Member, the Serra de Santa Helena Formation and the Lagoa do Jacaré Formation, waning on the top of this formation. Both carbon and strontium isotope ratios became decoupled from the global seawater curve, attesting for the restricted nature of the basin during the MIBE. After peak nutrient input, all TE concentrations plunge in pyrites from the Serra de Santa Helena and Lagoa do Jacaré formations, in line with other proxies that suggest the attainment of sulfate-poor and nutrient-depleted conditions that hampered the development of typical late Ediacaran/early Cambrian ecosystems in the interior basins of western Gondwana. However, while Se/Co ratios indicate a plunge of O<sub>2</sub> levels to below 1% in the Serra de Santa Helena Formation, those levels progressively increase to ca. 7% towards the younger samples of the Lagoa do Jacaré Formation. This might indicate a return to more ventilated conditions in the upper Bambuí Group. A re-connection with the global seawater during the early Cambrian is supported by the presence of tidal facies in the Lagoa do Jacaré Formation; by the abundance of diagenetic glauconite and phosphatic beds in the overlying Serra da Saudade Formation, dated at ca. 520 Ma, suggesting suboxic conditions and upwelling of deep nutrient-rich waters through the action of ressurgence; and the presence of *Treptchynus pedum* trace fossils on the Três Marias Formation, topmost unit of the Bambuí Group, indicating the return of favorable conditions for colonization of early Cambrian complex life forms.

## 5. Acknowledgments

This work is supported by Instituto Serrapilheira (Serra-1912-31510), Brazil, through Project MOBILE ([geolifemobile.com](http://geolifemobile.com)), by FAPEMIG, Brazil through the “Programa Pesquisador Mineiro” (PPM-00618-18), and by the Conselho Nacional de Desenvolvimento Científico e Tecnológico (CNPq, Brazil), through Universal grant nb. 408815/2021-3 and through Research Productivity Grant 304509/2021-3. A previous version was improved after comments and suggestions by three anonymous reviewers.

## 6. References

- Algeo, T. J., & Rowe, H., 2012. Paleoceanographic applications of trace-metal concentration data. *Chemical Geology*, 324-325, 6-18. doi:10.1016/j.chemgeo.2011.09.002
- Alvarenga, C.J.S., et al., 2014. Meso-Neoproterozoic isotope stratigraphy on carbonates platforms in the Brasilia Belt of Brazil. *Precambrian Res.* 251, 164–180.

- Blamey, N. J., Brand, U., Parnell, J., Spear, N., Lécuyer, C., Benison, K., ... & Ni, P. (2016). Paradigm shift in determining Neoproterozoic atmospheric oxygen. *Geology*, 44(8), 651-654.
- Caetano-Filho, S., Sansjofre, P., Ader, M., Paula-Santos, G. M., Guacaneme, C., Babinski, M., ... Trindade, R. I. F. (2021). A large epeiric methanogenic Bambuí sea in the core of Gondwana supercontinent? *Geoscience Frontiers*. doi:10.1016/j.gsf.2020.04.005
- Campbell, I.H. and Squire, R.J., 2010. The mountains that triggered the Late Neoproterozoic increase in oxygen: the Second Great Oxidation Event. *Geochimica et Cosmochimica Acta*, 74(15), pp.4187-4206.
- Cannell, A., Blamey, N., Brand, U., Escapa, I., & Large, R. (2022). A revised sedimentary pyrite proxy for atmospheric oxygen in the paleozoic: Evaluation for the Silurian-Devonian-Carboniferous period and the relationship of the results to the observed biosphere record. *Earth-Science Reviews*, 104062.
- Caxito F.A., Lana C., Frei R., Uhlein G.J., Sial A.N., Dantas E.L., Pinto A.G., Campos F.C., Galvão P., Warren L.V., Okubo J., Ganade C.E. 2021. Goldilocks at the dawn of complex life: mountains might have damaged Ediacaran–Cambrian ecosystems and prompted an early Cambrian greenhouse world. *Scientific Reports*, 11:20010. <https://doi.org/10.1038/s41598-021-99526-z>
- Caxito, F. A., Frei, R., Sial, A. N., Uhlein, G. J., Lima de Moura, W. A., Pereira, E., & Rodrigues, R. (2023). Chromium isotopes track redox fluctuations in Proterozoic successions of the Chapada Diamantina, São Francisco craton, Brazil. *Geology*, 51(1), 69-74.
- Caxito, F.A., et al., 2018. Multiproxy geochemical and isotope stratigraphy records of a Neoproterozoic Oxygenation Event in the Ediacaran Sete Lagoas cap carbonate, Bambuí Group, Brazil. *Chem. Geol.* 481, 119–132. <https://doi.org/10.1016/j.chemgeo.2018.02.007>.
- Caxito, F.A., Halverson, G.P., Uhlein, A., Stevenson, R., Dias, T.G., Uhlein, G.J., 2012. Marinoan glaciation in east central Brazil. *Precambrian Res.* 200–203, 38–58. <https://doi.org/10.1016/j.precamres.2012.01.005>.
- Crockford, P.W., et al., 2018. Linking paleocontinents through triple oxygen isotope anomalies. *Geology* 46 (2), 179–182. <https://doi.org/10.1130/G39470.1>.
- Cui, H. et al. Global or regional? Constraining the origins of the middle Bambuí carbon cycle anomaly in Brazil. *Precambrian Res.* 348, 105861 (2020).
- Dantas M.V.S., Uhlein A., Uhlein G.J., Freitas A.R., Mendonça T.K., Santos J.A.O., Silva S.A.M. Carbonate storm deposits and C, O isotopes of the Lagoa do Jacaré Formation (Ediacaran) in the Paraopeba area, Bambuí Group, Brazil. *Brazilian Journal of Geology*, 52(1):e20200135, 2022. <https://doi.org/10.1590/2317-4889202120200135>.
- Danyushevsky, L., Robinson, P., Gilbert, S., Norman, M., Large, R., McGoldrick, P., & Shelley, M. (2011). Routine quantitative multi-element analysis of sulphide minerals by laser ablation ICP-MS: Standard development and consideration of matrix effects. *Geochemistry: Exploration, Environment, Analysis*, 11(1), 51–60. doi:10.1144/1467-7873/09-244
- Fraga-Ferreira, P. L., Ader, M., Caetano-Filho, S., Sansjofre, P., Paula-Santos, G. M., Babinski, M., ... & Trindade, R. I. (2021). The Nitrogen Cycle in an epeiric sea in the core of Gondwana

Supercontinent: a study on the Ediacaran-Cambrian Bambuí Group, east-central Brazil. *Frontiers in Earth Science*, 678.

Freitas A.R., Uhlein A., Dantas M.V.S., Mendonça T.K. 2021. Caracterização em multiescala de carbonatos neoproterozóicos da Pedreira GMD, Formação Lagoa do Jacaré, Grupo Bambuí, Paraopeba-MG. *Geologia USP. Série Científica*, 21(1):103-120. <https://doi.org/10.11606/issn.2316-9095.v21-163573>.

Gilbert, S. E., Danyushevsky, L. V., Rodemann, T., Shimizu, N., Gurenko, A., Meffre, S., ... Death, D. (2014). Optimisation of laser parameters for the analysis of sulfur isotopes in sulphide minerals by laser ablation ICP-MS. *J. Anal. At. Spectrom.*, 29(6), 1042–1051. doi:10.1039/c4ja00011k.

Gregory D. D., Large R. R., Halpin J. A., Baturina E. L., Lyons T. W., Wu S., Danyushevsky L., Sack P. J., Chappaz A. and Maslennikov V. V. (2015) Trace element content of sedimentary pyrite in black shales. *Econ. Geol.* 110, 1389–1410.

Gregory D. D., Large R. R., Stepanov A. S. (2022). Ground-truthing the pyrite trace element proxy in modern euxinic settings. *Am. Mineral.* 107, 848-859.

Gregory, D., Perea, D., Taylor, S., Kovarik, L., Owens, J., and Lyons, T. (2019) The formation of pyrite frambooids: A view from TEM and APT. Goldschmidt, Barcelona, Spain, August, 18–23.

Guacaneme, C., Babinski, M., Bedoya-Rueda, C., Paula-Santos, G. M., Caetano-Filho, S., Kuchenbecker, M., ... & Trindade, R. I. (2021). Tectonically-induced strontium isotope changes in ancient restricted seas: The case of the Ediacaran-Cambrian Bambui foreland basin system, east Brazil. *Gondwana Research*, 93, 275-290.

Guacaneme, C., Caetano-Filho, S., Paula-Santos, G.H., Babinski, M., Fraga-Ferreira, P., Bedoya-Rueda, C., Kuchenbecker, M., Reis, H., Trindade, R., 2022. Paleoenvironmental redox evolution of Ediacaran-Cambrian restricted seas in the core of West Gondwana: Insights from trace-metal geochemistry and stratigraphy of the Bambuí Group, east Brazil. *Journal of South American Earth Sciences* 119, 103998, <https://doi.org/10.1016/j.jsames.2022.103998>.

Halverson, G. P., Wade, B. P., Hurtgen, M. T., & Barovich, K. M. (2010). Neoproterozoic chemostratigraphy. *Precambrian Research*, 182(4), 337–350. doi:10.1016/j.precamres.2010.04.007.

Hippertt, J.P., et al., 2019. The fate of a Neoproterozoic intracratonic marine basin: trace elements, TOC and IRON speciation geochemistry of the Bambuí Basin, Brazil. *Precambrian Res.* 330, 101–120. <https://doi.org/10.1016/J.PRECAMRES.2019.05.001>. Elsevier.

Huerta-Diaz, M. A., and Morse, J. W., 1992. Pyritization of trace metals in anoxic marine sediments. *Geochimica et Cosmochimica Acta* 56, 2681–2702.

Isotta, C., Rocha-Campos, A. & Yoshida, R. Striated Pavement of the Upper Pre-Cambrian Glaciation in Brazil. *Nature* 222, 466–468 (1969).

Jochum, K. P., Nohl, U., Herwig, K., Lammel, E., Stoll, B., & Hofmann, A. W. (2005). *GeoReM*: A New Geochemical Database for Reference Materials and Isotopic

Standards. *Geostandards and Geoanalytical Research*, 29(3), 333–338. doi:10.1111/j.1751-908x.2005.tb00904.x

Kuchenbecker, M., Babinski, M., Pedrosa-Soares, A.C., Lopes-Silva, L., Pimenta, F., et al., 2016. Chemostratigraphy of the lower Bambuí Group, southwestern São Francisco Craton, Brazil: insights on Gondwana paleoenvironments. *Braz. J. Geol.* 46 (Suppl. 1), 145–162. <https://doi.org/10.1590/2317-488920160030285>. Sociedade Brasileira de Geologia.

Kuchenbecker, M., Pedrosa-Soares, A. C., Babinski, M., Siqueira Reis, H. L., Atman, D., & Diniz da Costa, R. (2020). Towards an integrated tectonic model for the interaction between the Bambuí Group and the adjoining orogenic belts: Evidences from the detrital zircon record of syn-orogenic units. *Journal of South American Earth Sciences*, 102831.

Kulikov, E.A., Medvedev, I.P. Variability of the Baltic Sea level and floods in the Gulf of Finland. *Oceanology* 53, 145–151 (2013). <https://doi.org/10.1134/S0001437013020094>

Kulp, T. R., & Pratt, L. M. (2004). Speciation and weathering of selenium in upper cretaceous chalk and shale from South Dakota and Wyoming, USA. *Geochimica et Cosmochimica Acta*, 68(18), 3687–3701. doi:10.1016/j.gca.2004.03.008

Large, R. R., Danyushevsky, L., Hollit, C., Maslennikov, V., Meffre, S., Gilbert, S., Bull, S., Scott, R., Emsbo, P., Thomas, H., Singh, B., and Foster, J. (2009) Gold and trace element zonation in pyrite using a laser imaging technique: Implications for the timing of gold in orogenic and Carlin-style sediment-hosted deposits. *Economic Geology* 104, 635–668.

Large, R. R., Halpin, J. A., Danyushevsky, L. V., Maslennikov, V. V., Bull, S. W., Long, J. A., Gregory, D. D., Lounejeva, E., Lyons, T. W., and Sack, P. J. (2014) Trace element content of sedimentary pyrite as a new proxy for deep-time ocean–atmosphere evolution. *Earth and Planetary Science Letters* 389, 209–220.

Large, R. R., Halpin, J. A., Lounejeva, E., Danyushevsky, L. V., Maslennikov, V. V., Gregory, D., Sack, P. J., Haines, P. W., Long, J. A., and Makoundi, C. (2015) Cycles of nutrient trace elements in the Phanerozoic ocean. *Gondwana Research* 28, 1282–1293.

Large, R. R., Maslennikov, V. V., Robert, F., Danyushevsky, L. V., and Chang, Z.S. (2007) Multistage sedimentary and metamorphic origin of pyrite and gold in the giant Sukhoi Log deposit, Lena gold province, Russia. *Economic Geology* 102, 1233–1267.

Large, R. R., Mukherjee, I., Gregory, D., Steadman, J., Corkrey, R., & Danyushevsky, L. V. (2019). Atmosphere oxygen cycling through the Proterozoic and Phanerozoic. *Mineralium Deposita*, 54(4), 485-506.

Large, R. R., Mukherjee, I., Zhukova, I., Corkrey, R., Stepanov, A., & Danyushevsky, L. V. (2018). Role of upper-most crustal composition in the evolution of the Precambrian ocean–atmosphere system. *Earth and Planetary Science Letters*, 487, 44-53.

Large, R., Mukherjee, I., Gregory, D., Steadman, J., Danyushevsky, L., Corkrey, R. (2022). Sedimentary Pyrite Proxy for Atmospheric Oxygen; Evaluation of Strengths and Limitations. *Earth-science reviews* 227, 103941.

- Levyant, A. S., Rabinovich, B. I., and Rabinovich, A. B. (1994). Computation of seiche oscillations in seas of arbitrary configuration (exemplified by the Caspian Sea). *Oceanology* 33, 588–598.
- Lyons, T. W., Werne, J. P., Hollander, D. J., & Murray, R. W. (2003). Contrasting sulfur geochemistry and Fe/Al and Mo/Al ratios across the last oxic-to-anoxic transition in the Cariaco Basin, Venezuela. *Chemical Geology*, 195(1-4), 131-157.
- Medvedev IP, Rabinovich AB and Kulikov EA (2016) Tides in Three Enclosed Basins: The Baltic, Black, and Caspian Seas. *Front. Mar. Sci.* 3:46. doi: 10.3389/fmars.2016.00046
- Moreira D.S., Uhlein A., Dussin I.A., Uhlein G.J., Misuzaki A.M.P. 2020. A Cambrian age for the upper Bambuí Group, Brazil, supported by the first U-Pb dating of volcanioclastic bed. *Journal of South American Earth Sciences*, 99:102503. <https://doi.org/10.1016/j.jsames.2020.102503>.
- Moreira, M., Díaz, R., Santos, H., Mendoza, U., Böttcher, M., Capilla, R., Albuquerque, A.L., Machado, M., 2018. Sedimentary trace element sinks in a tropical upwelling system. *Journal of Soils and Sediments* 18, 287-296. <https://doi.org/10.1007/s11368-017-1803-4>
- Moura S.A., Uhlein A., Uhlein G.J., Dantas M.V.S. High-resolution stratigraphy of peritidal microbial carbonates from the Lagoa do Jacaré Formation, Bambuí Group, north of Minas Gerais state, Brazil. *Brazilian Journal of Geology*, 52(2):e20210040, 2022. <https://doi.org/10.1590/2317-4889202120210040>.
- Mukherjee I., Large, R., Corkrey, R., Willink, R., and Stepanov, A. (2018b) How robust is sedimentary pyrite trace element geochemistry as a geochemical proxy? *Goldschmidt Abstracts* 2018, 1829.
- Mukherjee, I., & Large, R. R. (2016). Pyrite trace element chemistry of the Velkerri Formation, Roper Group, McArthur Basin: Evidence for atmospheric oxygenation during the Boring Billion. *Precambrian Research*, 281, 13-26.
- Mukherjee, I., & Large, R. R. (2020). Co-evolution of trace elements and life in Precambrian oceans: The pyrite edition. *Geology*, 48(10), 1018-1022.
- Mukherjee, I., and Large, R., 2017, Application of pyrite trace element chemistry to exploration for SEDEX style Zn-Pb deposits: McArthur Basin, Northern Territory, Australia: *Ore Geology Reviews*, v. 81, p. 1249–1270.
- Mukherjee, I., Large, R. R., Bull, S., Gregory, D. G., Stepanov, A. S., Ávila, J., ... & Corkrey, R. (2019). Pyrite trace-element and sulfur isotope geochemistry of paleo-mesoproterozoic McArthur Basin: Proxy for oxidative weathering. *American Mineralogist*, 104(9), 1256-1272.
- Mukherjee, I., Large, R. R., Corkrey, R., and Danyushevsky, L. V. (2018a) The Boring Billion, a slingshot for complex life on Earth. *Scientific Reports* 8, 4432.
- Murray, J. W. (1975). The interaction of cobalt with hydrous manganese dioxide. *Geochimica et Cosmochimica Acta*, 39(5), 635-647.

- Nobre-Lopes, J., 2002. Diagenesis of the dolomites hosting Zn/Ag mineral deposits in the Bambuí Group at Januária region (MG) (PhD thesis) Universidade de Campinas, Campinas, p. 183.
- Nozaki, Y., 2010. Elemental distribution: Overview, in Steele, J., Thorpe, S.A., Turekian, K.K., eds., Marine chemistry and geochemistry: A derivative of encyclopedia of ocean sciences, 2nd edition: Amsterdam, Elsevier/ Academic Press, p. 7–12.
- Okubo, J. et al. The sulfur isotopic consequence of seawater sulfate distillation preserved in the Neoproterozoic Sete Lagoas post-glacial carbonate, eastern Brazil. *Jornal of the Geological Society* (2022), 179 (4). <https://doi.org/10.1144/jgs2021-091>.
- Okubo, J., Muscente, A. D. D., Luvizotto, G. L. L., Uhlein, G. J. J. & Warren, L. V. V. Phosphogenesis, aragonite fan formation and seafloor environments following the Marinoan glaciation. *Precambrian Res.* 311, 24–36 (2018).
- Paula-Santos, G.M., Babinski, M., Kuchenbecker, M., Caetano-Filho, S., Trindade, R.I., Pedrosa-Soares, A.C., 2015. New evidence of an Ediacaran age for the Bambuí Group in southern São Francisco craton (eastern Brazil) from zircon U-Pb data and isotope chemostratigraphy: *Gondwana Research*, v. 28, p. 702–720.
- Paula-Santos, G.M., et al., 2017. Tracking connection and restriction of West Gondwana São Francisco Basin through isotope chemostratigraphy. *Gondw. Res.* 42, 280–305. Elsevier.
- Piper, D. Z., & Dean, W. E. (2002). Trace-element deposition in the Cariaco Basin, Venezuela Shelf, under sulfate-reducing conditions: A history of the local hydrography and global climate, 20 ka to the present (No. 1670). US Geological Survey.
- Reis, H. L. S., & Suss, J. F. (2016). Mixed carbonate–siliciclastic sedimentation in forebulge grabens: An example from the Ediacaran Bambuí Group, São Francisco Basin, Brazil. *Sedimentary Geology*, 339, 83–103. doi:10.1016/j.sedgeo.2016.04.004
- Sahoo, S. K., Planavsky, N. J., Kendall, B., Wang, X., Shi, X., Scott, C., ... & Jiang, G. (2012). Ocean oxygenation in the wake of the Marinoan glaciation. *Nature*, 489(7417), 546-549.
- Sanchez, E.A.M.; Uhlein, A.; Fairchild, T.R., 2021. *Treptichnus pedum* in the Três Marias Formation, south-central Brazil, and its implications for the Ediacaran-Cambrian transition in South America. *Journal of South American Earth Sciences*, v. 105, p. 102983, 2021.
- Scott, C., Lyons, T.W., Bekker, A., Shen, Y., Poulton, S.W., Chu, X., Anbar, A.D. (2008) Tracing the stepwise oxygenation of the Proterozoic ocean. *Nature* 452, 456–459.
- Shields, G.A., 2005. Neoproterozoic cap carbonates: a critical appraisal of existing models and the plume world hypothesis. *Terra Nova* 17 (4), 299–310. <https://doi.org/10.1111/j.1365-3121.2005.00638.x>.

Steadman J.A., Large R.R., Blamey N.J., Mukherjee I., Corkrey R., Danyushevsky, L.V., Maslennikov, V., Hollings, P., Garven, G., Brand U. and Lecuyer, C., 2020, Evidence for elevated and variable atmosphere oxygen in the Precambrian: *Precambrian Research*, V. 343, 105722.

Stepanov, A. S., Danyushevsky, L. V., Large, R. R., Mukherjee, I., & Zhukova, I. A. (2020). Deconvolution of the composition of fine-grained pyrite in sedimentary matrix by regression of time-resolved LA-ICP-MS data. *American Mineralogist*, 105(6), 820-832.

Stockdale, A., Davison, W., Zhang, H., & Hamilton-Taylor, J. (2010). The association of cobalt with iron and manganese (oxyhydr) oxides in marine sediment. *Aquatic Geochemistry*, 16(4), 575-585.

Tatzel, M., von Blanckenburg, F., Oelze, M. Bouchez, J., Hippler, D., 2017. Late Neoproterozoic seawater oxygenation by siliceous sponges. *Nature Communications* 8, 621. <https://doi.org/10.1038/s41467-017-00586-5>.

Tribouillard, N., Algeo, T.J., Lyons, T., Riboulleau, A., 2006. Trace metals as paleoredox and paleoproductivity proxies: An update. *Chemical Geology* 232, 12-32. <https://doi.org/10.1016/j.chemgeo.2006.02.012>.

Uhlein, G. J., Caxito, F. A., Frei, R., Uhlein, A., Sial, A. N., & Dantas, E. L. (2021). Microbially induced chromium isotope fractionation and trace elements behavior in lower Cambrian microbialites from the Jaíba Member, Bambuí Group, Brazil. *Geobiology*, 19(2), 125-146.

Uhlein, G.J., et al., 2017. Early to late Ediacaran conglomeratic wedges from a completere land basin cycle in the southwest São Francisco Craton, Bambuí Group, Brazil. *Precambrian Res.* 299, 101–116. <https://doi.org/10.1016/j.precamres.2017.07.020>.

Uhlein, G.J., et al., 2019. Ediacaran paleoenvironmental changes recorded in the mixed carbonate-siliciclastic Bambuí Basin, Brazil. *Palaeogeogr. Palaeoclimatol. Palaeoecol.* 517, 39–51.

Vieira, L.C., Trindade, R.I.F., Nogueira, A.C.R., Ader, M., 2007. Identification of a Sturtian cap carbonate in the Neoproterozoic Sete Lagoas carbonate platform, Bambuí Group, Brazil. *Comptes Rendus Geoscience* 339, 240–258.

Violante, A., Krishnamurti, G. S. R., & Pigna, M. (2007). Factors affecting the sorption-desorption of trace elements in soil environments In A. Violante, P.M. Huang, and G.M. Gadd, Eds., *Biophysico-Chemical Processes of Metals and Metalloids in Soil Environments*, p. 169–213. Wiley.10.1002/9780470175484.ch5

Warren, L.V., et al., 2014. The puzzle assembled: Ediacaran guide fossil Cloudina reveals an old proto-Gondwana seaway. *Geology* 42 (5), 391–394. <https://doi.org/10.1130/G35304.1>.

Zhu, Z., Campbell, I.H., Allen, C.M., Brocks, J.J. and Chen, B., 2022. The temporal distribution of Earth's supermountains and their potential link to the rise of atmospheric oxygen and biological evolution. *Earth and Planetary Science Letters*, 580, p.117391.

## 5. CONCLUSÃO

A um primeiro olhar, o que mais se destaca neste conjunto de dados é a mudança, de uma maneira geral, das concentrações de Mo e Se, estas bem radicais, e de Cu, Cd, Zn, Ni e Bi nas piritas presentes nos carbonatos de capa do Membro Pedro Leopoldo em relação às concentrações destes elementos nas piritas das Formações Serra de Santa Helena e Lagoa do Jacaré. A restrição progressiva da bacia, passando de uma totalmente conectada para uma bacia restrita, devido ao desenvolvimento dos cinturões de montanhas circundantes de idade Brasiliana ao redor do cráton do São Francisco (orógeno Brasília em 630-600 Ma, seguido pelo orógeno Araçuaí, em 560-540 Ma, e finalmente pelas colisões terminais do Gondwana em 540-500 Ma; Caxito et al., 2021) é provavelmente a principal causa de mudança paleoambiental. Nota-se também a diferença da amostra JJ1, um *chert*, em relação às outras amostras do Membro Pedro Leopoldo, já que ela se encontra enriquecida em Zn e relativamente depletada para os demais elementos químicos analisados. Nobre-Lopes (2002) discorre sobre uma mineralização de Zn nas rochas carbonáticas da região de Januária-MG, o que pode ser uma explicação possível, já que elementos como Ni, Co e Mo possuem concentrações depletadas em regiões próximas a fontes hidrotermais (Mukherjee & Large, 2017).

Os teores de TE de pirita sedimentar de folhelhos negros, siltitos, carbonatos e amostras de *chert* do Grupo Bambuí indicam condições paleoambientais radicalmente distintas. Os resultados indicam a importância da conexão e restrição da bacia para a concentração de TE, nas piritas, e a influência de forças externas, como a orogênese, que podem levar ao desenvolvimento ou destruição de ecossistemas marinhos complexos.

Em compilações de dados de folhelhos negros ao longo do tempo geológico, concentrações altas de Mo interpretadas como decorrentes de um aumento do intemperismo por oxidação ocorrem após ca. 551 Ma (Scott et al., 2008). As amostras de pirita do Membro Pedro Leopoldo estudadas neste trabalho mostram enriquecimentos semelhantes de Mo de várias centenas de ppm, porém estas foram depositadas anteriormente, há cerca de 635-600 Ma atrás (Caxito et al., 2021), indicando um importante, embora passageiro, pulso de oxigenação como consequência da glaciação Marinoana.

Ainda sobre o Mo, seus maiores teores foram encontrados nas piritas das amostras de folhelho negro da seção Holcim (HCX), que apresentam os maiores fatores de enriquecimento de Mo encontrados no Grupo Bambuí (cerca de 10 vezes os do Folhelho Australiano Pós-Arqueano - PAAS; Hippert et al., 2019). Trabalhos como Large et al., 2014 e Gregory et al., 2019 descobriram que as concentrações de pirita refletem as dos folhelhos negros hospedeiros,

fielmente identificando os mesmos eventos de oxigenação (Large et al., 2014; Gregory et al., 2019). Pode-se inferir que a grande taxa de oxidação do ambiente produziu um grande reservatório de elementos químicos dissolvidos nas águas imediatamente pós-glaciais, globalmente conectadas, onde o Membro Pedro Leopoldo foi depositado.

O carbonato do Mb. Pedro Leopoldo foi depositado em uma plataforma conectada ao mar global há 635-600 Ma, sob uma coluna de água estratificada composta por uma camada óxica rasa e camadas euxínicas profundas. As razões Se/Co indicam O<sub>2</sub> atmosférico relativamente uniforme após a glaciação Marinoana. Os *proxies* estudados indicam claramente condições oxigenadas após o degelo da Terra Bola de Neve; no entanto, a evidência global sugere que estes representam pulsos de oxigenação atmosférica transitórios e prolongados, e que a atmosfera da Terra só se tornaria unidirecionalmente oxigenada para níveis modernos muito mais tarde no início do Fanerozóico (Large et al., 2014; Large et al., 2015). De qualquer forma, as condições transitórias de oxigênio e nutrientes foram mantidas até o final do Ediacarano, quando a colonização de organismos biomínernalizantes como *Cloudina sp.* ocorreu conforme registrado no Membro Lagoa Santa, depositado há 585-540 Ma.

Na seção superior, no entanto, as condições paleoambientais mudaram radicalmente, levando a uma depleção dos TE em pirita sedimentar das Formações Serra de Santa Helena e Lagoa do Jacaré, do final do Ediacarano ao início do Cambriano. De acordo com outras *proxies* disponíveis, isso indica a restrição progressiva do Grupo Bambuí e a desconexão do oceano global pelo desenvolvimento dos cinturões brasileiros circundantes.

No entanto, enquanto as razões Se/Co indicam uma queda dos níveis de O<sub>2</sub> para menos de 1% na Formação Serra de Santa Helena, esses níveis aumentam progressivamente para 7% em direção às amostras mais jovens da Formação Lagoa do Jacaré. Isso pode indicar um retorno às condições mais oxigenadas no topo do Grupo Bambuí. Uma reconexão com a água do mar global durante o início do Cambriano é sustentada pela presença de fácies de maré na Formação Lagoa do Jacaré; pela abundância de camadas diagenéticas de glauconita na Formação Serra da Saudade sobrejacente, datada de 520 Ma, sugerindo condições subóxicas e ressurgência de águas profundas ricas em nutrientes pela ação da ressurgência; e a presença de vestígios fósseis de *Treptichynus pedum* (Sanchez et al., 2021) na Formação Três Marias, unidade mais alta do Grupo Bambuí, indicando o retorno de condições favoráveis à colonização de formas de vida complexas.

Em suma, os conjuntos de dados disponíveis indicam que após um pico de aporte de nutrientes coincidente com a fase principal da atividade orogênica nos cinturões circundantes, registrado na porção baixa a média do Membro Lagoa Santa, o Grupo Bambuí ficou estagnado

e dominado por condições anóxicas (ferruginosas), levando ao desenvolvimento do intervalo MIBE e ao desaparecimento de quaisquer formas de vida complexas durante a deposição do Membro Superior Lagoa Santa, da Formação Serra de Santa Helena e da porção inferior da Formação Lagoa do Jacaré. Então, na seção superior, a reconexão da bacia pode ter ocorrido, levando a condições mais oxigenadas e, finalmente, o retorno de formas de vida complexas como registrado por vestígios fósseis no topo da Formação Três Marias.

## 6. REFERÊNCIAS BIBLIOGRÁFICAS

- Algeo, T. J., & Rowe, H., 2012. Paleoceanographic applications of trace-metal concentration data. *Chemical Geology*, 324-325, 6-18. doi:10.1016/j.chemgeo.2011.09.002
- Allan, M.M., Yardley, B.W.D., Forbes, L.J., Shmulovich, K.I., Banks, D.A., Shepherd, T.J., 2005. Validation of LA-ICP-MS fluid inclusion analysis with synthetic fluid inclusions. *American Mineralogist* 90, 1767-1775.
- Alvarenga, C.J.S., et al., 2014. Meso-Neoproterozoic isotope stratigraphy on carbonates platforms in the Brasilia Belt of Brazil. *Precambrian Res.* 251, 164–180.
- Blamey, N. J., Brand, U., Parnell, J., Spear, N., Lécuyer, C., Benison, K., ... & Ni, P. (2016). Paradigm shift in determining Neoproterozoic atmospheric oxygen. *Geology*, 44(8), 651-654.
- Brandalise, Luiz Alberto, 1980. Projeto Sondagem Bambuí: Relatório Final.
- Caetano-Filho, S., Sansjofre, P., Ader, M., Paula-Santos, G. M., Guacaneme, C., Babinski, M., ... Trindade, R. I. F. (2021). A large epeiric methanogenic Bambuí sea in the core of Gondwana supercontinent? *Geoscience Frontiers*. doi:10.1016/j.gsf.2020.04.005
- Campbell, I.H. and Squire, R.J., 2010. The mountains that triggered the Late Neoproterozoic increase in oxygen: the Second Great Oxidation Event. *Geochimica et Cosmochimica Acta*, 74(15), pp.4187-4206.
- Cannell, A., Blamey, N., Brand, U., Escapa, I., & Large, R. (2022). A revised sedimentary pyrite proxy for atmospheric oxygen in the paleozoic: Evaluation for the Silurian-Devonian-Carboniferous period and the relationship of the results to the observed biosphere record. *Earth-Science Reviews*, 104062.
- Caxito F.A., Lana C., Frei R., Uhlein G.J., Sial A.N., Dantas E.L., Pinto A.G., Campos F.C., Galvão P., Warren L.V., Okubo J., Ganade C.E. 2021. Goldilocks at the dawn of complex life: mountains might have damaged Ediacaran–Cambrian ecosystems and prompted an early Cambrian greenhouse world. *Scientific Reports*, 11:20010. <https://doi.org/10.1038/s41598-021-99526-z>
- Caxito, F. A., Frei, R., Sial, A. N., Uhlein, G. J., Lima de Moura, W. A., Pereira, E., & Rodrigues, R. (2023). Chromium isotopes track redox fluctuations in Proterozoic successions of the Chapada Diamantina, São Francisco craton, Brazil. *Geology*, 51(1), 69-74.
- Caxito, F.A., et al., 2018. Multiproxy geochemical and isotope stratigraphy records of a Neoproterozoic Oxygenation Event in the Ediacaran Sete Lagoas cap carbonate, Bambuí Group, Brazil. *Chem. Geol.* 481, 119–132. <https://doi.org/10.1016/j.chemgeo.2018.02.007>.
- Caxito, F.A., Halverson, G.P., Uhlein, A., Stevenson, R., Dias, T.G., Uhlein, G.J., 2012. Marinoan glaciation in east central Brazil. *Precambrian Res.* 200–203, 38–58. <https://doi.org/10.1016/j.precamres.2012.01.005>.
- Caxito, F.D.A., Uhlein, G.J., Uhlein, A., Pedrosa-Soares, A.C., Kuchenbecker, M., Reis, H., Sial, A.N., Ferreira, V.P., Alvarenga, C.J.S., Santos, R.V. and Vieira, L.C., 2019. Isotope stratigraphy of Precambrian sedimentary rocks from Brazil: Keys to unlock Earth's

hydrosphere, biosphere, tectonic, and climate evolution. In *Stratigraphy & Timescales* (Vol. 4, pp. 73-132). Academic Press.

Crockford, P.W., et al., 2018. Linking paleocontinents through triple oxygen isotope anomalies. *Geology* 46 (2), 179–182. <https://doi.org/10.1130/G39470.1>.

Cui, H. et al. Global or regional? Constraining the origins of the middle Bambuí carbon cycle anomaly in Brazil. *Precambrian Res.* 348, 105861 (2020).

Dantas M.V.S., Uhlein A., Uhlein G.J., Freitas A.R., Mendonça T.K., Santos J.A.O., Silva S.A.M. Carbonate storm deposits and C, O isotopes of the Lagoa do Jacaré Formation (Ediacaran) in the Paraopeba area, Bambuí Group, Brazil. *Brazilian Journal of Geology*, 52(1):e20200135, 2022. <https://doi.org/10.1590/2317-4889202120200135>.

Danyushevsky, L., Robinson, P., Gilbert, S., Norman, M., Large, R., McGoldrick, P., & Shelley, M. (2011). Routine quantitative multi-element analysis of sulphide minerals by laser ablation ICP-MS: Standard development and consideration of matrix effects. *Geochemistry: Exploration, Environment, Analysis*, 11(1), 51–60. doi:10.1144/1467-7873/09-244

Fraga-Ferreira, P. L., Ader, M., Caetano-Filho, S., Sansjofre, P., Paula-Santos, G. M., Babinski, M., ... & Trindade, R. I. (2021). The Nitrogen Cycle in an epeiric sea in the core of Gondwana Supercontinent: a study on the Ediacaran-Cambrian Bambuí Group, east-central Brazil. *Frontiers in Earth Science*, 678.

Freitas A.R., Uhlein A., Dantas M.V.S., Mendonça T.K. 2021. Caracterização em multiescala de carbonatos neoproterozóicos da Pedreira GMD, Formação Lagoa do Jacaré, Grupo Bambuí, Paraopeba-MG. *Geologia USP. Série Científica*, 21(1):103-120. <https://doi.org/10.11606/issn.2316-9095.v21-163573>.

Gilbert, S. E., Danyushevsky, L. V., Rodemann, T., Shimizu, N., Gurenko, A., Meffre, S., ... Death, D. (2014). Optimisation of laser parameters for the analysis of sulfur isotopes in sulphide minerals by laser ablation ICP-MS. *J. Anal. At. Spectrom.*, 29(6), 1042–1051. doi:10.1039/c4ja00011k.

Gregory D. D., Large R. R., Halpin J. A., Baturina E. L., Lyons T. W., Wu S., Danyushevsky L., Sack P. J., Chappaz A. and Maslennikov V. V. (2015) Trace element content of sedimentary pyrite in black shales. *Econ. Geol.* 110, 1389–1410.

Gregory D. D., Large R. R., Stepanov A. S. (2022). Ground-truthing the pyrite trace element proxy in modern euxinic settings. *Am. Mineral.* 107, 848-859.

Gregory et al. (2015). Trace Element Content of Sedimentary Pyrite in Black Shales.

Gregory, D., Perea, D., Taylor, S., Kovarik, L., Owens, J., and Lyons, T. (2019) The formation of pyrite frambooids: A view from TEM and APT. Goldschmidt, Barcelona, Spain, August, 18–23.

Guacaneme, C., Babinski, M., Bedoya-Rueda, C., Paula-Santos, G. M., Caetano-Filho, S., Kuchenbecker, M., ... & Trindade, R. I. (2021). Tectonically-induced strontium isotope changes in ancient restricted seas: The case of the Ediacaran-Cambrian Bambui foreland basin system, east Brazil. *Gondwana Research*, 93, 275-290.

- Guacaneme, C., Caetano-Filho, S., Paula-Santos, G.H., Babinski, M., Fraga-Ferreira, P., Bedoya-Rueda, C., Kuchenbecker, M., Reis, H., Trindade, R., 2022. Paleoenvironmental redox evolution of Ediacaran-Cambrian restricted seas in the core of West Gondwana: Insights from trace-metal geochemistry and stratigraphy of the Bambuí Group, east Brazil. *Journal of South American Earth Sciences* 119, 103998, <https://doi.org/10.1016/j.jsames.2022.103998>.
- Halverson, G. P., Wade, B. P., Hurtgen, M. T., & Barovich, K. M. (2010). Neoproterozoic chemostratigraphy. *Precambrian Research*, 182(4), 337–350. doi:10.1016/j.precamres.2010.04.007.
- Hippertt, J. P., Caxito, F. A., Uhlein, G. J., Nalini, H. A., Sial, A. N., Abreu, A. T. D., & Nogueira, L.B. (2019). The fate of a Neoproterozoic intracratonic marine basin: Trace elements, TOC and
- Hippertt, J.P., et al., 2019. The fate of a Neoproterozoic intracratonic marine basin: trace elements, TOC and IRON speciation geochemistry of the Bambuí Basin, Brazil. *Precambrian Res.* 330, 101–120. <https://doi.org/10.1016/J.PRECAMRES.2019.05.001>. Elsevier.
- Huerta-Diaz, M. A., and Morse, J. W., 1992. Pyritization of trace metals in anoxic marine sediments. *Geochimica et Cosmochimica Acta* 56, 2681–2702.
- iron:implications for iron partitioning in continentally derived particulates. *Chem. Geol.* 214 (3–4), 209–221.
- ironspeciation geochemistry of the Bambuí Basin, Brazil. *Precambrian Research*, 330, 101-120.
- Isotta, C., Rocha-Campos, A. & Yoshida, R. Striated Pavement of the Upper Pre-Cambrian Glaciation in Brazil. *Nature* 222, 466–468 (1969).
- Jochum, K. P., Nohl, U., Herwig, K., Lammel, E., Stoll, B., & Hofmann, A. W. (2005). *GeoReM*: A New Geochemical Database for Reference Materials and Isotopic Standards. *Geostandards and Geoanalytical Research*, 29(3), 333–338. doi:10.1111/j.1751-908x.2005.tb00904.x
- Kuchenbecker, M., Babinski, M., Pedrosa-Soares, A.C., Lopes-Silva, L., Pimenta, F., et al., 2016. Chemostratigraphy of the lower Bambuí Group, southwestern São Francisco Craton, Brazil: insights on Gondwana paleoenvironments. *Braz. J. Geol.* 46 (Suppl. 1), 145–162. <https://doi.org/10.1590/2317-488920160030285>. Sociedade Brasileira de Geologia.
- Kuchenbecker, M., Pedrosa-Soares, A. C., Babinski, M., Siqueira Reis, H. L., Atman, D., & Diniz da Costa, R. (2020). Towards an integrated tectonic model for the interaction between the Bambuí Group and the adjoining orogenic belts: Evidences from the detrital zircon record of syn-orogenic units. *Journal of South American Earth Sciences*, 102831.
- Kulikov, E.A., Medvedev, I.P. Variability of the Baltic Sea level and floods in the Gulf of Finland. *Oceanology* 53, 145–151 (2013). <https://doi.org/10.1134/S0001437013020094>
- Kulp, T. R., & Pratt, L. M. (2004). Speciation and weathering of selenium in upper cretaceous chalk and shale from South Dakota and Wyoming, USA. *Geochimica et Cosmochimica Acta*, 68(18), 3687–3701. doi:10.1016/j.gca.2004.03.008
- Large et al. (2017). Ocean and Atmosphere Geochemical Proxies Derived from Trace Elements in Marine Pyrite: Implications for Ore Genesis in Sedimentary Basins.

- Large, R. R., Danyushevsky, L., Hollit, C., Maslennikov, V., Meffre, S., Gilbert, S., Bull, S., Scott, R., Emsbo, P., Thomas, H., Singh, B., and Foster, J. (2009) Gold and trace element zonation in pyrite using a laser imaging technique: Implications for the timing of gold in orogenic and Carlin-style sediment-hosted deposits. *Economic Geology* 104, 635–668.
- Large, R. R., Halpin, J. A., Danyushevsky, L. V., Maslennikov, V. V., Bull, S. W., Long, J. A., Gregory, D. D., Lounejeva, E., Lyons, T. W., and Sack, P. J. (2014) Trace element content of sedimentary pyrite as a new proxy for deep-time ocean–atmosphere evolution. *Earth and Planetary Science Letters* 389, 209–220.
- Large, R. R., Halpin, J. A., Lounejeva, E., Danyushevsky, L. V., Maslennikov, V. V., Gregory, D., Sack, P. J., Haines, P. W., Long, J. A., and Makoundi, C. (2015) Cycles of nutrient trace elements in the Phanerozoic ocean. *Gondwana Research* 28, 1282–1293.
- Large, R. R., Maslennikov, V. V., Robert, F., Danyushevsky, L. V., and Chang, Z.S. (2007) Multistage sedimentary and metamorphic origin of pyrite and gold in the giant Sukhoi Log deposit, Lena gold province, Russia. *Economic Geology* 102, 1233–1267.
- Large, R. R., Mukherjee, I., Gregory, D., Steadman, J., Corkrey, R., & Danyushevsky, L. V. (2019). Atmosphere oxygen cycling through the Proterozoic and Phanerozoic. *Mineralium Deposita*, 54(4), 485-506.
- Large, R. R., Mukherjee, I., Zhukova, I., Corkrey, R., Stepanov, A., & Danyushevsky, L. V. (2018). Role of upper-most crustal composition in the evolution of the Precambrian ocean–atmosphere system. *Earth and Planetary Science Letters*, 487, 44-53.
- Large, R., Mukherjee, I., Gregory, D., Steadman, J., Danyushevsky, L., Corkrey, R. (2022). Sedimentary Pyrite Proxy for Atmospheric Oxygen; Evaluation of Strengths and Limitations. *Earth-science reviews* 227, 103941.
- Levyant, A. S., Rabinovich, B. I., and Rabinovich, A. B. (1994). Computation of seiche oscillations in seas of arbitrary configuration (exemplified by the Caspian Sea). *Oceanology* 33, 588–598.
- Longerich, H.P., Jackson, S.E., and Günther, D. (1996) Laser ablation inductively coupled plasma mass spectrometric transient signal data acquisition and analyte concentration calculation. *Journal of Analytical Atomic Spectrometry*, 11, 899–904.
- Lyons, T. W., Werne, J. P., Hollander, D. J., & Murray, R. W. (2003). Contrasting sulfur geochemistry and Fe/Al and Mo/Al ratios across the last oxic-to-anoxic transition in the Cariaco Basin, Venezuela. *Chemical Geology*, 195(1-4), 131-157.
- Medvedev IP, Rabinovich AB and Kulikov EA (2016) Tides in Three Enclosed Basins: The Baltic, Black, and Caspian Seas. *Front. Mar. Sci.* 3:46. doi: 10.3389/fmars.2016.00046
- Moreira D.S., Uhlein A., Dussin I.A., Uhlein G.J., Misuzaki A.M.P. 2020. A Cambrian age for the upper Bambuí Group, Brazil, supported by the first U-Pb dating of volcaniclastic bed. *Journal of South American Earth Sciences*, 99:102503. <https://doi.org/10.1016/j.jsames.2020.102503>.

Moreira, M., Díaz, R., Santos, H., Mendoza, U., Böttcher, M., Capilla, R., Albuquerque, A.L., Machado, M., 2018. Sedimentary trace element sinks in a tropical upwelling system. *Journal of Soils and Sediments* 18, 287-296. <https://doi.org/10.1007/s11368-017-1803-4>

Moura S.A., Uhlein A., Uhlein G.J., Dantas M.V.S. High-resolution stratigraphy of peritidal microbial carbonates from the Lagoa do Jacaré Formation, Bambuí Group, north of Minas Gerais state, Brazil. *Brazilian Journal of Geology*, 52(2):e20210040, 2022. <https://doi.org/10.1590/2317-4889202120210040>.

Mukherjee I., Large, R., Corkrey, R., Willink, R., and Stepanov, A. (2018b) How robust is sedimentary pyrite trace element geochemistry as a geochemical proxy? *Goldschmidt Abstracts* 2018, 1829.

Mukherjee, I., & Large, R. R. (2016). Pyrite trace element chemistry of the Velkerri Formation, Roper Group, McArthur Basin: Evidence for atmospheric oxygenation during the Boring Billion. *Precambrian Research*, 281, 13-26.

Mukherjee, I., & Large, R. R. (2020). Co-evolution of trace elements and life in Precambrian oceans: The pyrite edition. *Geology*, 48(10), 1018-1022.

Mukherjee, I., and Large, R., 2017, Application of pyrite trace element chemistry to exploration for SEDEX style Zn-Pb deposits: McArthur Basin, Northern Territory, Australia: *Ore Geology Reviews*, v. 81, p. 1249–1270.

Mukherjee, I., Large, R. R., Bull, S., Gregory, D. G., Stepanov, A. S., Ávila, J., ... & Corkrey, R. (2019). Pyrite trace-element and sulfur isotope geochemistry of paleo-mesoproterozoic McArthur Basin: Proxy for oxidative weathering. *American Mineralogist*, 104(9), 1256-1272.

Mukherjee, I., Large, R. R., Corkrey, R., and Danyushevsky, L. V. (2018a) The Boring Billion, a slingshot for complex life on Earth. *Scientific Reports* 8, 4432.

Murray, J. W. (1975). The interaction of cobalt with hydrous manganese dioxide. *Geochimica et Cosmochimica Acta*, 39(5), 635-647.

Nobre-Lopes, J., 2002. Diagenesis of the dolomites hosting Zn/Ag mineral deposits in the Bambuí Group at Januária region (MG) (PhD thesis) Universidade de Campinas, Campinas, p. 183.

Nozaki, Y., 2010, Elemental distribution: Overview, in Steele, J., Thorpe, S.A., Turekian, K.K., eds., *Marine chemistry and geochemistry: A derivative of encyclopedia of ocean sciences*, 2nd edition: Amsterdam, Elsevier/ Academic Press, p. 7–12.

Okubo, J. et al. The sulfur isotopic consequence of seawater sulfate distillation preserved in the Neoproterozoic Sete Lagoas post-glacial carbonate, eastern Brazil. *Jornal of the Geological Society* (2022), 179 (4). <https://doi.org/10.1144/jgs2021-091>.

Okubo, J., Muscente, A. D. D., Luvizotto, G. L. L., Uhlein, G. J. J. & Warren, L. V. V. Phosphogenesis, aragonite fan formation and seafloor environments following the Marinoan glaciation. *Precambrian Res.* 311, 24–36 (2018).

Paula-Santos, G.M., Babinski, M., Kuchenbecker, M., Caetano-Filho, S., Trindade, R.I., Pedrosa-Soares, A.C., 2015, New evidence of an Ediacaran age for the Bambuí Group in

- southern São Francisco craton (eastern Brazil) from zircon U-Pb data and isotope chemostratigraphy: *Gondwana Research*, v. 28, p. 702–720.
- Paula-Santos, G.M., et al., 2017. Tracking connection and restriction of West Gondwana São Francisco Basin through isotope chemostratigraphy. *Gondw. Res.* 42, 280–305. Elsevier.
- Piper, D. Z., & Dean, W. E. (2002). Trace-element deposition in the Cariaco Basin, Venezuela Shelf, under sulfate-reducing conditions: A history of the local hydrography and global climate, 20 ka to the present (No. 1670). US Geological Survey.
- Poulton, S.W., Canfield, D.E., 2005. Development of a sequential extraction procedure for
- Reis, H. L. S., & Suss, J. F. (2016). Mixed carbonate–siliciclastic sedimentation in forebulge grabens: An example from the Ediacaran Bambuí Group, São Francisco Basin, Brazil. *Sedimentary Geology*, 339, 83–103. doi:10.1016/j.sedgeo.2016.04.004
- Sahoo, S. K., Planavsky, N. J., Kendall, B., Wang, X., Shi, X., Scott, C., ... & Jiang, G. (2012). Ocean oxygenation in the wake of the Marinoan glaciation. *Nature*, 489(7417), 546-549.
- Sanchez, E.A.M.; Uhlein, A.; Fairchild, T.R., 2021. *Treptichnus pedum* in the Três Marias Formation, south-central Brazil, and its implications for the Ediacaran-Cambrian transition in South America. *Journal of South American Earth Sciences*, v. 105, p. 102983, 2021.
- Scott, C., Lyons, T.W., Bekker, A., Shen, Y., Poulton, S.W., Chu, X., Anbar, A.D. (2008) Tracing the stepwise oxygenation of the Proterozoic ocean. *Nature* 452, 456–459.
- Shields, G.A., 2005. Neoproterozoic cap carbonates: a critical appraisal of existing models and the plumeworld hypothesis. *Terra Nova* 17 (4), 299–310. <https://doi.org/10.1111/j.1365-3121.2005.00638.x>.
- Steadman J.A., Large R.R., Blamey N.J., Mukherjee I., Corkrey R., Danyushevsky, L.V., Maslennikov, V., Hollings, P., Garven, G., Brand U. and Lecuyer, C., 2020, Evidence for elevated and variable atmosphere oxygen in the Precambrian: *Precambrian Research*, V. 343, 105722.
- Stepanov, A. S., Danyushevsky, L. V., Large, R. R., Mukherjee, I., & Zhukova, I. A. (2020). Deconvolution of the composition of fine-grained pyrite in sedimentary matrix by regression of time-resolved LA-ICP-MS data. *American Mineralogist*, 105(6), 820-832.
- Stockdale, A., Davison, W., Zhang, H., & Hamilton-Taylor, J. (2010). The association of cobalt with iron and manganese (oxyhydr) oxides in marine sediment. *Aquatic Geochemistry*, 16(4), 575-585.

Tatzel, M., von Blanckenburg, F., Oelze, M. Bouchez, J., Hippler, D., 2017. Late Neoproterozoic seawater oxygenation by siliceous sponges. *Nature Communications* 8, 621. <https://doi.org/10.1038/s41467-017-00586-5>.

Tribouillard, N., Algeo, T.J., Lyons, T., Riboulleau, A., 2006. Trace metals as paleoredox and paleoproductivity proxies: An update. *Chemical Geology* 232, 12-32. <https://doi.org/10.1016/j.chemgeo.2006.02.012>.

Uhlein, G. J., Caxito, F. A., Frei, R., Uhlein, A., Sial, A. N., & Dantas, E. L., 2021. Microbially induced chromium isotope fractionation and trace elements behavior in lower Cambrian microbialites from the Jaíba Member, Bambuí Group, Brazil. *Geobiology*, 19(2), 125-146.

Uhlein, G.J., et al., 2017. Early to late Ediacaran conglomeratic wedges from a complete foreland basin cycle in the southwest São Francisco Craton, Bambuí Group, Brazil. *Precambrian Res.* 299, 101–116. <https://doi.org/10.1016/j.precamres.2017.07.020>.

Uhlein, G.J., et al., 2019. Ediacaran paleoenvironmental changes recorded in the mixed carbonate-siliciclastic Bambuí Basin, Brazil. *Palaeogeogr. Palaeoclimatol. Palaeoecol.* 517, 39–51.

Vieira, L.C., Trindade, R.I.F., Nogueira, A.C.R., Ader, M., 2007. Identification of a Sturtian cap carbonate in the Neoproterozoic Sete Lagoas carbonate platform, Bambuí Group, Brazil. *Comptes Rendus Geoscience* 339, 240–258.

Violante, A., Krishnamurti, G. S. R., & Pigna, M., 2007. Factors affecting the sorption-desorption of trace elements in soil environments In A. Violante, P.M. Huang, and G.M. Gadd, Eds., *Biophysico-Chemical Processes of Metals and Metalloids in Soil Environments*, p. 169–213. Wiley. [10.1002/9780470175484.ch5](https://doi.org/10.1002/9780470175484.ch5)

Warren, L.V., et al., 2014. The puzzle assembled: Ediacaran guide fossil Cloudina reveals an old proto-Gondwana seaway. *Geology* 42 (5), 391–394. <https://doi.org/10.1130/G35304.1>.

Zhu, Z., Campbell, I.H., Allen, C.M., Brocks, J.J. and Chen, B., 2022. The temporal distribution of Earth's supermountains and their potential link to the rise of atmospheric oxygen and biological evolution. *Earth and Planetary Science Letters*, 580, p.117391.